Photocatalytic Potential of Biogenic Silver Nanoparticles and its Process Optimization for Methylene Blue Decolorization

A

Dissertation Report

Submitted in Partial Fulfillment of the Requirements

For the Award of the Degree of

Master of Science

in

Biotechnology

Garima Sharma

Registration no. 301601026

Under the Supervision of:

Dr. Shekhar Agnihotri

Department of Biotechnology

TIET, Patiala

June 2018

CERTIFICATE

This is to certify that dissertation entitled **"Photocatalytic Potential of Biogenic Silver Nanoparticles and its Process Optimization for Methylene Blue Decolorization"** submitted by Ms. Garima Sharma in partial fulfillment of the requirement for the award of the degree of **Master of Science** in Department of Biotechnology, TIET, Patiala (India) is the record of the candidate's own independent and original research work carried out under our supervision and guidance. The matter embodied in this dissertation has not been submitted in part to any other University/Institute for the award of any degree or diploma in India.

08/06/2018

Dr. Shekhar Agnihotri
Supervisor
Assistant Professor
Department of Biotechnology
TIET, Patiala- 147004

Dr. Moushumi Ghosh
Proessor & Head
Department of Biotechnology
TIET, Patiala Patiala (Punjab) India

DECLARATION

I hereby declare that the work which is being presented in dissertation entitled **"Photocatalytic Potential of Biogenic Silver Nanoparticles and Its Process Optimization for Methylene Blue Decolorization"** submitted by me for the award of the degree of **Master of Science** in Department of Biotechnology, TIET University, Patiala is true and original record of my own independent and original research work carried out under the supervision of Dr. Shekhar Agnihotri. Further, I declare that no part of this dissertation has been submitted to any other University/Institute for the award of any degree in India or abroad.

Place: Patiala

Date:

8/6/18

Garima Sharma

ACKNOWLEDGEMENT

I have taken efforts in this project. However, it would not have been possible without the kind support and help of many individuals and organization. I would like to extend my sincere thanks to all of them.

I am highly obligated to my guide **Dr. Shekhar Agnihotri** for their guidance and constant supervision as well as for providing necessary information regarding the project & also for their support in completing the project.I would like to express my gratitude towards all the research scholars **Mr. Devendra Sillu**, **Ms. Navneet Kaur**, **Ms. Anjali Chauhan**for their kind co-operation and encouragement which help me in the completion of this project.I would also like to express my special thanks to my lab mates **Ms. Suborna Chatterjee**, **Ms. Isha Rani** for giving me thoughtful advices and motivation to do my work with precision.

I wish to express my heartfelt gratitude towards **Mr Naminder** for their timely help and incessant cooperation during this project. My thanks and appreciations also go to my colleague**Ms. Vanita Kinra**, **Ms. Simran Mehta,** whose joyful company kept me alive throughout out my entire stay at Thapar. They willingly helped me out with their abilities in each situation.

I would like to mention the unconditional support from my family, whose blessings boosted me to achieve my destination. My loving thanks to my father **Mr. Rakesh Sharma**, my mother **Mrs. Gayatri Sharma**, my elder sister **Ms. Ridhima Sharma** and my younger brother **Mr. Devansh Sharma**.

Place: Patiala

Date: 8/6/18

Garima Sharma

Table of Contents

LIST OF TABLES

LIST OF FIGURES

LIST OF ABBREVIATIONS

Ag^+	Silver ions
AgNO3	Silver nitrate
AgNPs	Silver nanoparticles
AuNPs	Gold nanoparticles
CB	Conduction Band
DLS	Dynamic Light Scattering
FTIR	Fourier Transform Infra-red Spectrum
MB	Methylene Blue
mM	Milli molar
nm	Nanometer
NP	Nanoparticle
OD	Optical Density
pH	Potential of hydrogen
ppm	parts per million
RSM	Response Surface Methodology
SnO_2	Tin dioxide
SPR	Surface Plasmon Resonance
TiO_2	Titanium Dioxide
UV	Ultra- violet
VB	Valence Band
ZnO	Zinc Oxide

ABSTRACT

Due to the exponential growth of industries in recent years, there is intensification in the release of dyes directly into environment, hence resulting in water pollution, which detriments the human as well as aquatic life. Therefore, reliable and impactful solution is required to deal with this problem. Different physical and chemical methods are used to degrade the dyes, like ultrafiltration, electrochemical destruction, membrane filtration, ozonation etc. Nanoparticles grabbed the attention of scientists as nanoparticles have unique physical, chemical and optical properties from its bulk counterpart, and hencecan be utilized for different applications. Chemical as well as physical methods for nanoparticle synthesis are toxic and are not feasible, but the biogenic synthesis is eco-friendly, cheap and efficient. In this study, rapid biogenic synthesis of silver nanoparticles (AgNPs) from pineapple peel waste (*Ananas comosus*) is reported. The core size of synthesized AgNPs is 14-42 nm as depicted from characterization, established by UV- Vis spectroscopy, dynamic light scattering (DLS), fourier- transform infrared spectroscopy (FT-IR). Moreover, decolorization of pollutant dye- Methylene blue was undertaken in direct sunlight to study the photocatalytic potential of biogenically synthesized AgNPs. Optimization for the photocatalytic reaction was done with the Response Surface Methodology (RSM) andsilver nanoparticles demonstrated with efficient decolorization of (MB) methylene blue within few hours. The decolorization of dye was confirmed by UV- Vis spectrophotometric analysis with a decrease in absorbance of MB at 664 nm with respect to time. Biogenic Ag Nps efficiently degrades MB dye upto 98.04±0.23% within 173 min of exposure time. Even biogenic Ag NPs shows prominent anti-bacterial activity against *Pseudomonas aeruginosa* and *Bacillus subtilis*. These results clarify the application of biogenic Ag NPs synthesized by *Ananas comosus* in wastewater plants, textile industries and also in pharmaceutical industries.

CHAPTER 1

Introduction

In the modern world, water pollution has emerged as one of the most serious issue which is adversely affecting human and other species. Out of several sources of water pollution, industries related to chemical processing such as textile generate a large portion of dye effluents while processing and treating fabrics (Malik and Grohmann, 2012). This is inevitable since the textile industries contribute a huge proportion of the economy of countries worldwide. Particularly, after China, India is the largest exporter of dyestuffs i.e. where ~80% of the chemicals are involved in making dyestuffs and pigments. This amount is close to around 80,000 tons (Mathur, 2006, Sahoo et al 2013). The annual production of synthetic dyes through the globe is ~10^6 tons, out of which 1-1.5 x 10^5 tons are discharged directly into the wastewaters either untreated or after primary treatment (Zollinger, 1989, Singh, 2017).

Most of the dyes are organic in nature, and synthetic dyes are commonly utilized in the field of new technology, for example, in different types of paper, textile, leather tanning, plastics, food processing, rubber, cosmetics, dye manufacturing, and printing industries(Bensalah et al 2009). Even the synthetic dyes are used for tracing the ground water, for specifically determination of a particular area of sewage, activated sludge, wastewater treatment,etc (Hsu and Chiang, 1997). Methylene blue belongs to the class of thiazine dyes. It is organic and water soluble dye that is commonly used to dye wool, cotton, silk, and acrylic fibers, but when used carelessly, it can cause serious problems. MB is not highly poisonous, but it can cause burning eyes or may lead to permanent damage to human and animal eyes (Tan et al. 2007). It can also cause breathing difficulties and may result in symptoms like vomiting, nausea, gastritis,profuse sweating, diarrhea as well as mental confusion on inhalation (Abd EI-Latif et al. 2010). It is cationic in nature, and they are more lethal than negatively charged dyes (anionic dyes) (Hao et al. 2000). Discharge of MB into the hydrosphere signifies the major reason for the pollution due to its nature of recalcitrance. The unwanted layer of dye over the water surface, reduces the penetration of sunlight and therefore resist the photochemical and biological action to aquatic life. In the recent data, 100,000 and more dyes are identified with the production of 7 x 10^5tons/ year (Yagub et al.

2012). Around 100 tons of dyes are discharged into water bodies per annum. Basically, the accurate data of the discharge of dyes from different procedures in the environment are still not known.

The organic dyes are composed of petroleum with mineral derived components. The first organic dye made by humans was mauveine. Organic dyes impose serious problems to our environment due to its toxic nature. Many industries like textile, medicines, plastics, etc. use the organic dyes, and the waste from these industries directly goes into water bodies, which results in toxicity. Around 10-15 % of the total dye content addsup to the water bodies making it unpleasant and highly colored. The amassing of dyes in the water bodies causes eutrophication, which is directly affecting the reoxygenation capacity and causes greater harm to the aquatic system. An organic dye in the water bodies also inhibits the sunlight to reach inside the system and hence affect the water ecosystem (Faisal et al 2007).

Various approaches have been explored so far regarding the effective degradation or decolorization of dyes. For instance, various treatments like ultrafiltration, electrochemical techniques, and adsorption though have shown an initial success, they were found inadequate to remove dye content from aqueous ecosystem completely. Therefore, there is an utmost requirement for new technologies which could show promising results as the effect of light, pH, and the microbial attack is not enough to treat the dye pollution (Pagga, 1994). With the advent of nano-enabled hybrid technologies, the researchers have gained some practical relevance of treating textile wastewater over conventional methods. The use of nanotechnology in this problem has more advantages such as no formation of polycyclic products,quick oxidation, and also oxidation of pollutants. It is one of the effective and rapid techniques for the treatment of water bodies (Sobana et al 2006).

Nanoparticles consist of distinctive properties as compared to its bulk part, which includes unique mechanical, optical, physical, and the electromagnetic properties. There are other metal nanoparticles like TiO_2, ZnO and other oxides. The size, large surface area to volume ratio, shape, and mass dependent activity made metal nanoparticles, highly photocatalytic in nature (Ghosh et al., 2002). TiO_2 has been studied widely due to its stability and has shown excellent results, but it only works under UV irradiation as it only absorbs UV light. A well-known fact that UV radiations are only 10% of the solar spectrum, hence; it is a

crucial drawback in TiO_2 based photo-catalysis in direct sunlight (Wu et al., 2010). Other types of nanoparticles are also being used, i.e. gold and silver. As well as silver nanoparticles possess significant roles in biology like in the field of therapeutics (antiviral, antimicrobial, antiparasitic, anticancer, antioxidant and antidiabetic activities), drug delivery, agriculture, food production, waste treatment (G. et al., 2018).

Nanotechnology based on colloids has been established to regulate the shape, size, functionality and uniformity. Among various routes of nanoparticle synthesis, chemical methods have gained the highest applicability due to its robustness, ease, and better control on morphology, size and dispersity. However, many times the involvement of toxic reducing agents during chemical synthesis may pose a serious risk to the system and in turn the entire ecosystem. Therefore, biogenic synthesis has gained special attention over a past few years where nanoparticles are synthesized using biogenic reductants such as plant extracts, protein, amino acid, citric acid and other biochemical products which are safe, environment friendly and pose no significant toxicity (Rokhade and Taranath, 2017). For a strong upcoming nanotechnology, strategy of green chemistry should be implemented for the synthesis of nanoparticles by using renewable and eco-friendly methods to degrade dangerous organic solvents and chemical reducing agents (Anon, 2018). The biosynthesized AgNPs from plant source exhibits high degradation/decolorization action under a source of visible light. Among various plant source, *Ananas comosus* (pineapple) is a tropical fruit, which is known to be highly rich in vitamin C. Pineapple also contains bromelain (proteolytic enzyme) that helps in digestion of proteins. The pineapple peel waste also contains a very high amount of phenolic and antioxidant compounds which may behave as reducing agents for the synthesis of silver nanoparticles.

Therefore, in the recent study, an effort was made to synthesis silver nanoparticles using pineapple peel extract and later the biogenic nanoparticles were used to decolorize methylene blue (MB) dye. Synthesized nanoparticles are characterized through UV-Visible spectroscopy, Fourier Transform Infrared Spectroscopy (FTIR), and Dynamic Light Scattering (DLS) for nanoparticle morphology, size, and size distribution. The photocatalytic activity of biogenic AgNPs is done varying four different parameters, pH, dye concentration, AgNPs concentration, and time.Response Surface Methodology is a strong tool that is utilized to reduce the number of experiments which is required to provide enough information for

acceptable results. Hence, this method is less time consuming and laborious in comparison to full experimental runs. Basically, RSM is used to find most important variables that are directly affecting the experiment so that, those variables can be manipulated in order to accomplish optimum results. Therefore, the optimization of process parameters is done through Response Surface methodology (RSM) exhibiting the maximum extent of dyedecolorization.

Objectives of the project work

- Synthesis of (Ag NPs) silver nanoparticles utilizing natural reducing agents, i.e. plant extract and characterization.
- Evaluation of the effect of various process parameters on morphology of synthesized silver nanoparticles.
- Determining the efficiency of dye decolorization and optimization of the various condition parameters using Response Surface Methodology (RSM).

CHAPTER 2

Literature Review

Dyes can be generally classified into two major categories, Organic and Synthetic dyes. Synthetic dyes are most commonly used in industrial sector, according to their particular applications (Bensalah et al 2009). Dyes that are commonly used in recent days are safranin, Congo red, methylene blue, eosin, methyl orange, etc., they are basically composed of petroleum with mineral derived components. The first dye made by humans was mauveine, after that day numerous classes of dyes have been developed. Based on the charge carried by the dye molecule they can be cationic or anionic in nature, where cationic dyes are known to be comparatively lethal than their anionic counterpart (Hao et al. 2000). MB is an organic dye that belongs to the class of thiazine dyes. It is water soluble and is commonly used to dye wool, cotton, silk, and acrylic fibers. The excessive use of MB can cause burning eyes or may lead to permanent damage to eyes (Tan et al. 2007). In some cases, it can also cause breathing difficulties and may result in symptoms like vomiting, nausea, gastritis,profuse sweating, diarrhea also mental confusion on inhalation (Abd EI-Latif et al. 2010). For the sake of environment and social safety it is very vital to eradicate dyes from the water bodies via any way possible.

Various approaches have been explored by researchers so far regarding the effective degradation/decolorization of dyes which includes physical, chemical and biological methods. For instance, in physical method various treatments are involved like adsorption, peat, ultrafiltration, membrane filtration, ion exchange, wood chips, etc. Although they have shown initial success, but are limitedly used due to their declined efficiency in aqueous ecosystem and economical aspect when used at large scale. Chemical methods include electrochemical destruction, ozonation, photochemical, Fentons reagent method, etc., these methods are also held back by the same obstacle as physical methods. Biological methods on the other hand include, Adsorption by living/dead microbial biomass, Decolorisation by white-rot fungi, etc. Though these methods are environment friendly as well as economical, but require significant amount of time to act on dyes, sometimes up to a few days thus making the process time consuming and infeasible. Therefore, there is an utmost requirement

for new technologies which would show promising results as compared to the conventionally used methods (Tan et al, 2013).

In the recent times, with the advent of Nano-enabled hybrid technologies, the researchers have gained some practical relevance of treating polluted wastewater over conventional methods.

2.1 Nanotechnology

Nanotechnology is the science that deals with the objects at Nano scale which is further useful in the real world. The specific chemical and physical properties of nanomaterial is exploited and used for social assistance. The field of nanotechnology is interdisciplinary at higher extent and is still developing (Bhushan, n.d.). On 29 December 1959, the concept behind this technology started with a talk by American Physicist Richard Feynman, named "There's Plenty of Room at the Bottom" at the Technology Institute of California. In this talk, he explained how scientists can control or manipulate the individual molecules or atoms. Richard Feynman was also honored by the title of "Father of Nanotechnology". After the period of a decade, the term "Nanotechnology" was coined by Professor Norio Taniguch (Nano.gov, 2018). Bio nanotechnology is one of the emerging fields of nanotechnology, which is based on chemical pathways and principles of living organisms. This field works upon the relation between nanotechnology and the molecular biology- regulating the development of apparatus at Nano scale via the function and structure of natural Nano-techniques that are already established in the living cells (trynano.org, 2018). In recent times, nanotechnology has remarkable applications at industrial level. For example, nanotechnology has profound influence on medical machineries like imaging probes, diagnostic biosensors, and systems of drug delivery in the pharmaceutical companies. In cosmetics and food industries too the nanotechnology is used for improvements in shelf life, packaging, production, and bioavailability. Even the nanoparticles are used for checking and detecting the food safety and quality. There are many and diverse potential benefits of nanotechnology. The high exposure to nanoparticles also imposes some serious aspects about Nano toxicology. It is the study of potential health effects by nanoparticles. Nanomaterial's also have impending benefits in the field of medicines like improved drug delivery system, reduced inflammations, antibacterial coating over medical devices, improved surgical healing

of tissue, and detection of cancer cells in blood circulation. But due to the lack of complete information about the toxicology of nanomaterials, the potential use of nanotechnology is subdued.

2.2 Properties of Nanoparticles

The size of particle has direct impact on the chemical as well as physical properties of the particle. When the molecule size is in Nano scale, it behaves totally different from their bulk counterpart. Also thesurface molecules are higher in number and hence the greater number of dangling bonds. The greater is dangling bonds greater is the free energy of surface. Therefore, it is dynamically favorable for stable structure to lower the number of dangling bonds and thereby reducing the surface free energy. Nanoparticles behave like individual atoms due to the formation of discrete energy level rather than the continuum energy levels.The decline in particle size of bulk to Nano range effectsthe proportion of surface energy by increasing it and also the reduces the internal spacing.There is a decrease in the melting point with respect to reduction in particle size.Optical properties vary with the change in size of the component.Decrease in size of particle also increases band gap which results in the shift of light absorption towards the high energy region (blue shift) (Viswanathan, 2009).The energy gap also increases when the particle size reduces, and hence the conductivity reduces.Reduction of material at Nano scale can also increase its fatigue strength up to 250%.After a reduction in particle size, there is an increase in surface area and the availability of the reactant molecules increased, therefore increase in catalytic activity.

2.3 Nanoparticles Synthesis

Synthesis of nanoparticles includes the major two approaches:

1. Top down approach – In this approach bulk material breakdown into the smaller ones
2. Bottom up approach – In this approach the smaller atoms allowed to aggregate to form larger particles/ molecules.

Owing to control on dispersity, size and shape of nanoparticle, bottom up approaches are always preferred over top down approaches. Within bottom-up approach, synthetic methods for nanoparticle synthesis can broadly be classified under physical, chemical, biological.

Chemical methods are simple and cheap, even self-patterning and assembly is possible by this method. The nanoparticles are generally “colloid” in nature which is synthesized by chemical methods. Some of the chemical methods include, sol-gel method, solution based synthesis. In physical method, there are 2 types of techniques that are mechanical and vapor. Mechanical technique includes, melt mixing, and ball milling. And the vapor technique includes, laser ablation, ion implantation; sputter deposition, physical vapor deposition and electric arc deposition. In biological method,fungi, algae, plants, DNA etc. can be utilized for the nanoparticle synthesis. Biological method is simple, non-toxic, and cheap. All other methods comprise the consumption of noxious chemicals, but the method of green synthesis from plant extracts shows eco-friendly nature and simple methodology (Ramalingam et al. 2014; Muthukrishnan et al. 2015; Singh et al. 2013; Kanipandian et al. 2014)

2.4 Biogenic Synthesis of Nanoparticles

There are various biogenic sources for the metallic and other nanoparticles synthesis which includes plant, bacteria,algae, fungi, etc. But the use of plants for the synthesis of silver nanoparticles (Ag NPs) has focused attention, because of non-pathogenic, economical protocol,eco-friendly, and a technique with single step for the biogenic processes. Whereas, plants are best option because they are cost efficient and need no maintenance. In plants different parts can be used to synthesize nanoparticles like roots, bark, fruit, stem, seeds and leaves. Plants are basically “chemical factories” of nature as they comprise the large amount of secondary metabolites. These secondary metabolites have redox capacity and can be used for synthesis of nanoparticles. There are various numbers of metabolites present in plant sources, the synthesis rate is also higher as compared to microorganisms and synthesized nanoparticles from plant source are much more stable. In past, substantial studies on the synthesis of metal nanoparticles from plant extracts were reported, which would impact the future of downstream processing and plant tissue culture in order to synthesis metal nanoparticles at large scale in industries. As silver shows the highest band intensity of surface plasmon resonance, hence, synthesis of (Ag NPs) silver nanoparticles gain more attention. Numerous plants are utilized to synthesize silver nanoparticles, some of the examples are *Capsicum annum*(K. Jha and Prasad, 2011), *Solanum muricatum*(Gorbe et al., 2016), *Leea*

indica(Anon, 2017), and*Emblica officinalis*(Palanisamy et al., 2014). Some other studies are shown in the table below:

Table 1: Biogenic synthesis of various types of nanoparticles from different plant sources

NP Type	***Source Plant***	***Plant Part***	***Reference***
TiO_2 NPs	*Prunus × yedoensis* (Yoshino Cherry)	Leaf	Manikandan et al., 2017
Au NPs	*Marsilea quadrifolia*	Leaf	Chowdhury et al., 2017
Ag NPs	*Ziziphus Jujuba*	Leaf	Gavade et al., 2015
Ag NPs	*Bougainvillea spectabilis*	Flower	Pareek et al, 2012
SnO_2 NPs	*Saraca indica* (Ashoka Tree)	Flower	Vidhu et al, 2015
ZnO NPs	*RutaGraveolens* (Common rue)	Stem	Lingaraju et al., 2015
Ag NPs	*Pedalium murex*	Leaf	Anandalakshmi et al, 2015
Ag NPs	*Musa acuminata (*Banana)	Peel	Ibrahim, 2015
Ag NPs	*Jatropha curcas*	Latex	Bar et al., 2009
Ag NPs	*Aloe indica Royle*(Aloe Vera)	Leaf	Murugan et al., 2015
Ag NPs	*O. tenuiflorum* (Holy Basil)	Leaf	Logeswari et al. 2015

* NPs- Nanoparticles, Ag- Silver, Au- Gold, ZnO- Zinc oxide, TiO_2- Titanium oxide, SnO_2- Tin dioxide

2.5 Factors Affecting the Biogenic Synthesis

I. Species of microorganism/ plant: Each species have different types of reducing agents, so different species can form different sizes of particles. Even the morphology can vary from species to species.

II. Concentration of $AgNO_3$: Higher is the concentration of silver nitrate; higher is the chances of aggregation and formation of bulkier particles.

III. Concentration of extracts: Higher is the concentration, more is the availability of capping and reducing agents.

IV. Temperature: Higher temperature leads to high rate of chemical kinetics, and temperature also affects the size distribution of the particles.

2.6 Nanomaterials in Photocatalysis

To degrade the pollutants in an environment different methods are adopted, photocatalysis is one of the attention gaining technique. The aqueous system of nature is mostly purified by sunlight that initiates the breakdown of organic compounds into simpler forms, CO_2 and other mineral acids. As the decolorization of organic compounds does not produce any toxic compounds, therefore it is the main advantage of the photocatalytic procedure over other existing technologies and there is also no further necessity for disposal methods (Beydoun et al., 1999). In photocatalysis costly oxidizing agents are not needed as an ambient oxygen acts as an oxidant. The feature of a model photocatalyst is that, it should be non-toxic,stable, inexpensive as well as highly photoactive. Nanoparticles act as a photocatalyst, which enhances the reaction of photocatalysis. Silver nanoparticles absorb the light in the visible range and hence have more value in photocatalytic decolorization of organic dyes in water bodies. When silver salt added with plant extract, (Ag^+) silver ions reduced to form (Ag^0)silver atoms, those atoms clustered to form the nanoparticles. In plants various reducing agents are present like glycosides, alkaloids, phenols, polyols, carbohydrates, vitamin C, flavonoids, amino acids, etc. Some binding sources are also required, which can coat the silver nanoparticles and prevent further clustering of the atoms. Binding or stabilizing agents include citrate, $NaBH_4$, sodium citrate etc. The size range that generally desired is 20-50 nm.

In nanoparticles, combined oscillations of electrons of conduction band results in Surface Plasmon Resonance (SPR), and these electrons resonate with the incident light (electromagnetic field). When these electrons settle to their thermal equilibrium states, they release heat in their surroundings which induce reaction in molecules that are adhered on the surface of nanoparticles. In silver NPs there is interband transition of 4d electrons to 5sp electrons, which is responsible for the substantial UV light absorption. Therefore, they act as potential photocatalyst that has capability to use full solar spectrum. Silver NP enhances photocatalytic activity by causing charge separation and produces electron-hole pairs, on the surface of electron donors and semiconductors.Dye decolorization is directly dependent on the active oxidation species (AOS) formation. For example, AgNPs have band gap of approx.

3eV (Gharibshahi et al., 2017), when irradiated under UV radiation or direct sunlight, electrons jump from the valence to the conduction band, which results in formation of positively charged holes and electrons hence leading to the generation of AOS that is responsible for decolorization of dyes. The ability of AgNPs for charge separation prevents the recombination of holes and electrons; hence AOS formed remain stable to degrade dyes. Another mechanism for the decolorization of the dye was also reported, which states that solar radiations are much more effective than any other source of irradiation (Kansal et al 2008; Kumar et al., 2013). When the photons strike to the NPs, electrons gets excited and the oxygen molecules in the reaction mixture accept these excited electrons and there is generation of anion radicals of oxygen (Yu et al., 2012). These radicals then degrade the dye into simpler molecules from complex organic molecules (Ameta et al., 2012), hence AgNPs are stable and effective photocatalystunder the solar irradiation Vanaja M. et al (2014).

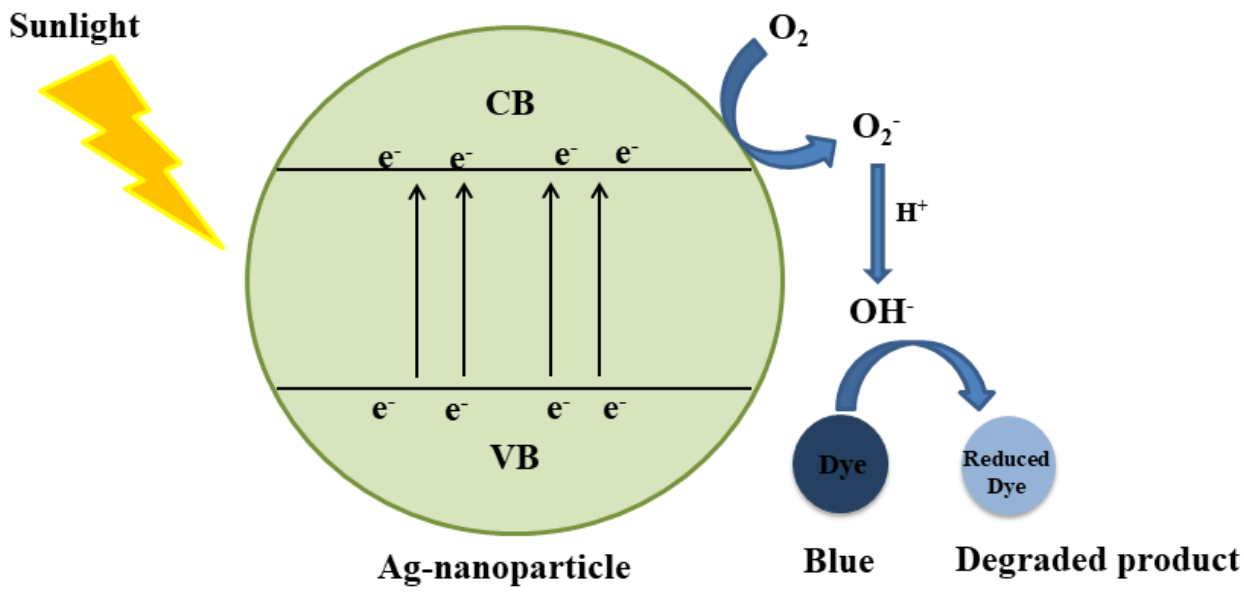

Figure 1: Mechanism of decolorization of dye with silver nanoparticles

There are various literatures showing the ion and decolorization of methylene blue (MB) dye by silver nanoparticles. For instance, AgNPs are synthesized from *Morinda tinctoria* leaf extract which degrades 95% of MB dye in 72 hours (Vanaja M. et al 2014), *Casuarina equisetifolia* leaf extract also used to synthesize AgNPs which degrades 37% in 5 hours (Saranya V.T. K.et al. 2016). There is size difference of AgNPs in both the cases, (as shown

in the table below) this signifies that size affects the decolorization rate of the dye. As small size of NPs results in large potential difference, this increases the rate of reduction (Veisi et al 2018). Furthermore, small size of NPs provides large surface-to-volume ratiothat is more molecules on the surface and it acts as catalytic sites.

Table 2: Various dye decolorization by different types of nanoparticles

NPs type	***Synthesis method***	***NP size***	***Dye decolorization %***	***Reference***
AgNPs	Biogenic (Plant-*Morinda tinctoria*)	79-96 nm	MB, 95% in 72 hours	Vanaja et al (2014)
AgNPs	Biogenic (Plant-*Casuarina equisetifolia*)	9-22 nm	MB, 37% in 5 hours	Saranya. et al. (2016)
AgNPs	Biogenic (Yeast-*Saccharomyces cerevisiae*)	10 nm	MB, 85% in 6 hours	Roy et al (2014)
AgNPs	Biogenic (Plant-*Helicteres isora*)	30-40 nm	Eosin MB, 95% in 3 hours	Bhakya.et al (2015)
AgNPs	Biogenic (Plant- *Hypnea musciformis)*	2–55.8 nm	MO, 95% in 10 hours	Ganapathy et al (2014)
AuNPs	Biogenic (Chitosan)	17 nm	p-Nitrophenol, 95% in 17 min	Wu et al (2015)
TiO_2 NPs	Chemical	<500 nm	MV, 69% in 15 min	Saeed et al (2017)
TiO_2 NPs	Chemical	14-21 nm	Safranin, 80% in 70 min	Khalyavka et al (2016)
Ag-TiO_2 NPs	Chemical	2-10 nm	Safranin-O, 96% in 70 min	El-Kemary et al (2015)
Doped-TiO_2 NPs	Chemical	80-100 nm	MV, 82.4 % in 3 hours	Yang et al (2013)
AgNPs	Biogenic (Plant)	60-80 nm	CV, >99.9% in 2 hours	Farhan et al (2015)

* NP- Nanoparticles, Ag-Silver, MB-Methylene Blue, MV- Methyl violet, MO- Methyl orange, CV-Crystal violet

Even yeast *Saccharomyces cerevisiae*used to synthesize AgNPs, which is futher used to degrade MB dye. Yeast extract degrades the MB upto 86% in only 6 hours (Roy K. et al 2014). Various other dyes are also degraded by the utilization of AgNPs like methyl orange (Ganapathy S. G. et al 2014), crystal violet (Farhan M. A. et al 2015). Moreover, the concentration of NP used to degrade the dye effects the rate of decolorization, for example, when catalyst (AgNPs synthesized by *Helicteres isora*)dose increased from 20 to 100 μg/mL there was an increase in decolorizationrate upto 100% of dye eosin methylene blue (Bhakya S.et al 2015).Recyclability of the AgNPs were reported for the decolorizationof three dyes (MB, Rhodamine B, and 4-nitrophenol), even after the 8 cycles of reaction substantial activity was maintained for the complete conversion of dyes(Veisi et al 2018).

2.7 Characterization techniques

2.7.1 UV-Vis Spectrophotometric Analysis

UV- Visible Spectroscopy is the one of the essential tool in the field of analytical chemistry. This is basically related to the interface between matter and light. As the light falls upon the matter, the electrons in atoms or molecules get excited from its ground state to higher excited state. So the concept is that the energy absorbed by radiations is equal to the difference of energy between the ground state and excited state. In UV- Vis Spectrophotometric Analysis, light absorption by the sample provides the information of electronic transitions going on in the material. It also helps in obtaining the optical band gap, as it analyses electronic transitions between conduction and valence band (Maes and Willems, 2011).The principle behind this technique is Beer- Lambert law; which explainsthat decrease in the rate of light intensity is directly proportional to the concentration of sample and incident light, when a beam with monochromatic light passes through a sample with an absorbing material.This method ensures the presence of nanoparticles by the peak formation at particular wavelength, due the surface plasmon resonance of nanoparticles (Amendola et al, 2009). Silver nanoparticles show peak absorbance between 390 nm to 420 nm; this reflects that the sizes of particles are in nano range i.e. between 10-100 nm.

2.7.2 Fourier-transform infrared spectroscopy (FTIR)

FTIR is an diagnostic technique that is constantly developing, which allows a non-destructive, rapid, high-throughput, reagentless analysis of various range of type of samples. It is basically a valuable tool for metabolic fingerprinting due to its ability to characterize amino acids, carbohydrates, lipids, proteins and polysaccharides. FTIR is adaptable technique as the sample requirement is much lower. Typically 0.5 – 20 µL of sample can be spotted on plates for analysis and data can be collected within seconds (Trenerry and Rochfort, 2012). The basic principle behind this technique is that most of the molecules absorb radiations of IR- region in electromagnetic spectrum. A molecular bond specifically corresponds to this absorption. The range of FT-IR is measured as wave number with the range of 4000-600 cm^{-1}. In this technique, IR spectrum of emission or absorption of gas, liquid or solid is obtained, as it collects high resolution data over wide range of spectra.

2.7.3 Dynamic light scattering (DLS)

Dynamic light scattering (DLS), aka Quasi-Elastic Light Scattering (QELS), is non-destructive and conventional technique to measure the size of particles, and even the size distribution among the sample typically in the range of submicron. In the recent technology the size lower than 1 nm can also be measured easily. It is basically used for characterization of emulsions, particles or molecules, which are dissolved or dispersed in liquid. The principle behind this technique is Brownian motion of molecules or particles in suspension scattered the laser of light at different intensities. Measurement of these fluctuations of intensities can be used to analyze the Brownian motion velocity and the size of particle by the Stoke-Einstein relationship (Bauer and Schnapp, 2012). In DLS, these fluctuations can be measured by photon counter. The fluctuation of intensity is directly proportional to the rate of molecular diffusion in the solvent, which is in turn related to hydrodynamic radii of particles. In the DLS, there is interaction between the particles and the light. With this technique, even the particle sizes within the narrow range (2 -500 nm) can be measured. Polydispersity of the sample can sometimes distort the expected results as big particles can screen the small particles.

2.7.4 Zeta Potential

Zeta potential can be defined as charge difference between the solid surface and the liquid around it. This potential value can be measured in millivolts. Potential difference may arise due to dissociation on the surface of ionogenic group or due to solution ions adsorption into the region of surface. Ion distribution is effected by the net charge on the surface of particle, due to which counter ions concentration increases near to the surface. Therefore, double layer of charge is formed at the interface of surface- liquid. Hence, zeta potential is a function of particle's surface charge, composition and nature of surrounding medium, and adsorbed layer around interface. Zeta potential results are useful in practical studies and to control the stability of collides and flocculation processes. It is associated with particles and biomolecules interactions and is an important factor for the aggregate formation. When any metal oxide NPs are dissolved in water, the value of zeta potential directly depends on the surface condition and the molecular species (Horie and Fujita, 2011). Value of zeta potential confirms the stability of emulsions. Higher value of zeta potential (positive or negative) means that particles in emulsion are stable and the lower value indicate that particles have the tendency to flocculate or coagulate, which means poor stability of particles in the emulsion. Basically, when the value of zeta potential is high it means repulsive forces are larger than the attractive forces, resulting in the stable system (Lu and Gao, 2010).

2.7.5 X-ray diffraction (XRD)

XRD is a fast systematic tool that is commonly used to identify the phase of crystalline substance and also provides the information about cell dimensions. The sample is finely grounded, mixed well in solvent (homogenized), and bulk composition is also determined. It is basically, depends upon the interference of X-rays and the sample; the source of X-rays is cathode ray tube, which generates the monochromatic light wave that directly concentrated on the sample. When the circumstances fulfill the Bragg's law, i.e. $n\lambda=2d \sin \theta$, then the constructive interference produced after the interaction between sample and incident rays. Bragg's law co-relates the parameters that are diffraction angle, wavelength of EM radiations, and the lattice spacing (Pandian, 2014). Unique "fingerprint" of the crystalline sample was obtained after the analysis with XRD, and the data from XRD can we used to depict the crystalline form after some comparisons with standard measurements and patterns.

2.7.6 Transmission electron microscopy (TEM)

TEM is the primary tool to analyze the internal structure of material at nanoscale. The transmission electron microscope has great impact in the material science. The principle behind this technique is that, electron beam with potential of 40-100 kV, passes through the thin layered sample. Commonly, its principle is same as that of light microscope, but beam of electron is used in place of light because electron beam has much lower wavelength than light, hence, images of TEM are much more precise than that of light microscope. Even the finest details of the structure can be analyzed by the TEM- sometimes as small as atoms (Howe et al 2012). It is used to examine the composition of layers, their growth and flaws in semiconductors. TEM have high resolution value that is about 0.2 nanometers. TEM has 3 essential parts: (1) an electron gun, and the condenser, which centers the electron beam on the sample, (2) image generating system that includes specimen stage, objective, projector lenses, which forms the real, enlarged image, and (3) system of image recording, which translates electron image to perceptible form (Anjum, 2016). With the help of TEM microstructures of viruses, organelles and molecules can be visualized with high resolution.

CHAPTER 3

Methodology

3.1 Materials

Silver nitrate ($AgNO_3$) was bought from Sigma-Aldrich Chemicals; Sodium Hydroxide (NaOH) pellets were also procured from Sigma-Aldrich's EMPLURA® range, Methylene Blue (MB) dye powder was obtained from SD Fine chemicals. The pineapple peel waste was collected from the local juice shop. Glasswares were washed with an Aqua regia solution and then cleaned three times with distilled water. All the glasswares were then oven dried at 60°C for 2 hours and then stored in a dry container for further use.

3.2 Preparation of Pineapple Peel Extract

Firstly, pineapple peel waste was cleaned with DI water and then dried in the dark, followed by grinding in the mixer. 30 g of grinded material and 300 ml of DI water was mixed and was heated at 60˚C for 30-40 min, afterwards; the mixture was allowed to rest at room temperature for cooling and then filtered through muslin cloth further followed by centrifugation at 5000 rpm for 10 min. The pellets were discarded and the supernatant was filtered again with 0.2µ membrane filter and stored at 4ºC until further use.

Figure 2: Dried pineapple peel

3.3 Biosynthesis of AgNPs

The synthesis of silver nanoparticles was carried out by adding 1 ml aqueous solution of $AgNO_3$ to 9ml of the pineapple peel waste extract and constantly stirring it at room temperature for 30 minutes.The instant change in color from light yellow to reddish brown signifies that the Ag NPs were formed.

To estimate the reduction capacity of pineapple peel waste extract and its effect on formed silver nanoparticles, different concentration of silver precursor i.e. silver nitrate were used. As shown in table 3, five varying concentrations of silver nitrate were prepared according to the concentration of final reaction solution as shown in table 4.

Table 3: Different concentration of silver nitrate solutions

Sample name	***$AgNO_3$(mg)***	***Water added(ml)***	***Final Conc. (Ag)***
A	0.85	1	~5 mM
B	1.7	1	~10 mM
C	2.4	1	~15 mM
D	8.5	1	~50 mM
E	15.3	1	~90 mM

Table 4: Different concentration of samples of silver nanoparticles

$AgNO_3$ Sample	***Extract vol. (ml)***	***$AgNO_3$ vol. (ml)***	***Conc. of Ag in solution (mM)***
A	9	1	0.5
B	9	1	1
C	9	1	1.5
D	9	1	5
E	9	1	9

To study the pH effect on silver nanoparticles synthesis, pH of the extract (pineapple peel waste) was adjusted at four different values, i.e. 4.0, 6.0, 8.0 and 10.0, then 9ml of extract was mixed with 1ml of solution B in 4 different glass vials of 15 ml. The glass vials were then incubated at room temperature for biogenic silver nanoparticles synthesis while

UV-Vis spectrophotometer readings were taken at intervals of time to measure the extent of formation of nanoparticles.

3.4 Preparation of MB Solution

A MB stock solution was prepared by mixing 2 mg of MB powder in 50 ml of distilled water and was stirred using a magnetic stirrer for 5 min. The working MB solutions were subsequently prepared over a wide range of 0.5-30 ppm (0.5, 1, 5, 10, 20, 30 ppm) from the stock solution of 40 ppm.

3.5 Photocatalytic decolorization of MB Dye

The photocatalytic decolorization of organic pollutant i.e.MB dye was done with the biogenic synthesized AgNPs. The reaction was carried out by mixing 2.8 ml MB dye with 200 µL of AgNPs (1mM) in different test tubes. Reaction mixtures were then allowed to stand in direct sunlight. The decolorization kinetics was studied using UV-Visspectrophotometer over 3 hour duration. The decolorization percentage calculated by the formula**;**

$$\text{Decolorization (\%)} = \frac{C_0 - C}{C_0} \times 100$$

Where, C- Final Concentration dye, and C_o- Initial concentration of dye.

3.6 Optimizationof dye decolorizationRSM

Single factor study

To determine the variable affecting the dye decolorization most single factor study was done. Four different factors were taken into consideration for the single factor effect on the decolorization of dye. These factors include (A) effect of pH, (B) effect of dye conc. (ppm), (C) effect of Ag NPs conc. (mM) and (D) effect of time.

(A) Effect of pH- 20 ppm dye solution was prepared, with five different pH, i.e. 3, 5, 7, 9, and 11 and 1mM AgNP solution was mixed with it. UV-Vis spectrophotometric readings were taken after 3 hours.

(B) Effect of dye conc.(ppm)- dye solution was prepared with four different conc., i.e. 10, 20, 30, and 40 ppm, pH was maintained at 7.0 and 1mM AgNP solution was mixed with it then the UV-Vis spectrophotometric readings were taken after 3 hours.

(C) Effect of Ag NPs conc.(mM)- 20 ppm dye solution was prepared with pH 7.0 and 3 ml of it taken into 5 different glass tubes. Ag NP solutions of different conc. i.e. 0.5, 1, 1.5, 5, and 9 mM were then mixed with the dye solution. UV-Vis spectrophotometric readings were taken after 3 hours.

(D) Effect of time- 20 ppm dye solution was prepared with 7.0 pH and 1 mM of AgNP solution was mixed with it. UV-Vis spectrophotometric readings were taken after 10, 20, 30, 45, 60, 90, and 180 min.

Statistical analysis

The Design Expert software (version 6.0.8, state-Ease Inc, Minnealpolis, USA) was employed for statistical analysis and to obtain the optimized parameters. In Response Surface Methodology (RSM) Box-Behnken design with 3 independent factors at three levels was utilized. The range of independent variables, namely, the pH of the solution, Initial Dye concentration (ppm), and irradiation time (min) in direct sunlight were chosen based on the preliminary experimentations. The factor level was coded as -1 (low), 0 (central point), and +1 (high) as shown table below.

Table 5: The levels and ranges of variables in Box–Behnken statistical experimental design.

Variable	Symbol	Coded level		
		Low	**Centre**	**High**
		-1	**0**	**+1**
pH	A	4	7	10
Dye Conc. (ppm)	B	10	25	40
Time (min)	C	10	95	180

The cubic model was found to be aliased, hence could not be used for modelling of the experimental data. Dye decolorization (%) was represented as a second order polynomial equation to express the effect of different varibles on the response:

$$Y = \beta_0 + \sum \beta_i X_i + \sum \beta_{ii} X_i^2 + \sum \beta_{ij} X_i X_j$$

Where Y= represents response, X_i and X_j= independent variables that affect the response. The β_0 defines regression coefficient for the intercept, β_i for linear, β_{ij} for cross product terms and β_{ii} for quadratic.

Analysis of Variance (ANOVA) was engaged to examine the model competence for observed responses by experiments. It is a arithmetic analytical tool to evaluate the enactment of tested experiments, by perceiving the value of"p", multiple correlation coefficients (R^2) , lack of fit,as well as adjusting coefficient of determination (R^2-adj). In this case, 17 different set of experiments plan were designed based on Box-Behnken design. The generated model by RSM was then validated by performing experiments at the generated optimum variblale condition.

Table 6:RSM based Box-Behnekn experimental design for independent variables

Run	pH	Dye conc.	Time
1	7.00	10.00	180.00
2	10.00	40.00	95.00
3	10.00	25.00	180.00
4	7.00	25.00	95.00
5	7.00	25.00	95.00
6	4.00	25.00	10.00
7	4.00	40.00	95.00
8	7.00	25.00	95.00
9	7.00	10.00	10.00
10	7.00	40.00	180.00
11	4.00	10.00	95.00
12	10.00	25.00	10.00
13	4.00	25.00	180.00
14	7.00	40.00	10.00
15	10.00	10.00	95.00
16	7.00	25.00	95.00
17	7.00	25.00	95.00

3.7 Kinetic Modeling

Photocatalytic decolorization of dye can be more precisely described by kinetic modeling, models are also known as decay models. For practical application of photocatalytic reaction, kinetic models are necessary (Chen, 1999). In this study, four different kinetic models were made to analyze the photocatalytic decolorization of MB by AgNPs.

1) First-order kinetic model (equation)

$$\ln[C_0\text{-}C] = - kt$$

2) Pseudo First-order kinetic model (equation)

$$\ln[C\text{-}C_0] = \ln[C] - kt$$

3) Second-order kinetic model (equation)

$$\frac{1}{C} - \frac{1}{C_0} = kt$$

4) Pseudo Second-order kinetic model (equation)

$$\frac{t}{C} = \frac{t}{C_0} - \frac{1}{kC^2}$$

3.8 Antimicrobial activity

The antimicrobial activity of biogenic Ag NPs was carried out by the method of well diffusion. Agar medium was prepared and autoclaved at 121º C, 15 psi for 1 hour. Agar poured in the plates and it was allowed to solidified, after which microbial lawns were prepared with 10^{-5} diluted culture. Two different microbial cultures were taken i.e. *Pseudomonas aeruginosa* (gram-negative) and *Bacillus subtilis* (gram-positive)The wells were bored on agar plates and the Ag NPs solution of concentration 1 mM added into it. Plates were then kept at 37 º C for 24 hours. Inhibition zones were then measured,experimentations were done in triplicates and the mean outcomes were presented.

CHAPTER 4

Results and Discussion

4.1 Characterization of Synthesized Nanoparticle

4.1.1 UV-Vis Spectrophotometric Analysis

Physiochemical factors like reaction time and pH variations were taken into account to optimize the synthesis of silver nanoparticles. The formation of Ag NPs was detected visually, as the sample color changes from light yellow to brownish color. UV-Vis spectroscopy was utilized to confirm the synthesis the silver nanoparticles. Absorption peak intensified in the range of 390- 420 nm, indicating the SPR band which confirms the production of AgNPs. The intensity of the color was increased progressively as the time duration of reaction increases. Time intervals that were chosen to measure the UV-Vis spectra of the given samples were 1 min, 10 min, 15 min, 20 min, and 30 min. After 24 hours, silver ions were reduced to the silver atoms and there is no further significant change in peak was observed, this shows that there was capping agents in the extracts that limits the further reaction in the sample.Silver ions reduced by plant components and forms silver atoms, these silver atoms clustered together to form the silver nanoparticles. Mechanism of Ag NPs formation is illustrated in the figure below.

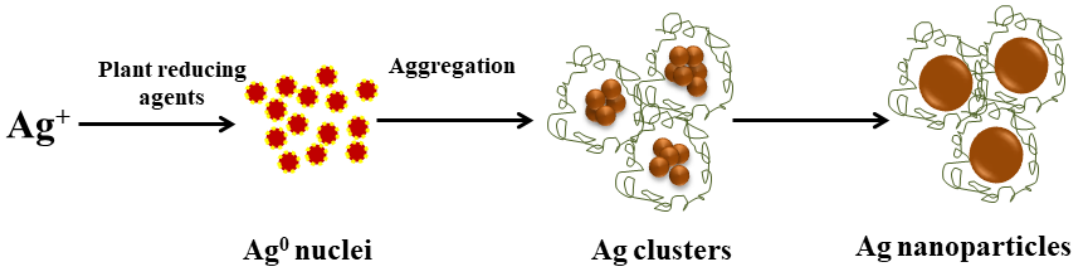

Figure 3: Mechanism of silver nanoparticles synthesis

Influence of pH on the silver nanoparticles synthesis was investigated using different pH of extract, i.e. pH 4.0, 6.0, 8.0, 10.0;the final concentration of silver was maintained at 1 mM. As shown in the graphs below, as the time increases the peak absorbance of extract

decreases (range 200-250 nm) and that of silver nano cluster increases (range 350-400 nm). Peak of silver nano clusters gets sharper with the passage of time.

There is formation of precipitates after 24 hour incubation of sample of pH 4, no precipitation is observed in the samples with pH 6, 8 and 10. Instant color change was observed in each sample at different pH.

There is rapid synthesis of AgNPs was observed at pH near 8.0, it is because of phenolic groups of plant extracts that gets ionized, whereas at acidic pH (4.0) AgNPs aggregates to form the larger NPs that gets settled and precipitation was observed. At the higher range of pH, larger number of AgNPs was synthesized with smaller sizes(Iravani and Zolfaghari, 2013). Mock et al evaluated that the size of nanoparticles varies with the fluctuations in pH (Mock et al., 2002). Veerasamy et al., found that with the elevated range of pH there is acceleration of nucleation, which results in large production of NPs with smaller diameter (Veerasamy et al., 2011). Conversely, at lower pH, AgNPs generally aggregates rather than nucleate. As the best peak absorbance was observed in the sample with pH 10.0, hence further studies were done over the range of pH 10.

The pineapple peel waste extract was mixed with various amounts of silver nitrate to form the silver nanoparticles of different concentrations i.e., 0.5 mM, 1 mM, 1.5 mM, 5 mM, and 9 mM. Color was observed as the silver nanoparticles absorb the energy from the visible region of the electromagnetic spectrum. On Shimadzu UV–visible spectrophotometer (UV-2600), absorbance was recorded in range of 200-800 nm.

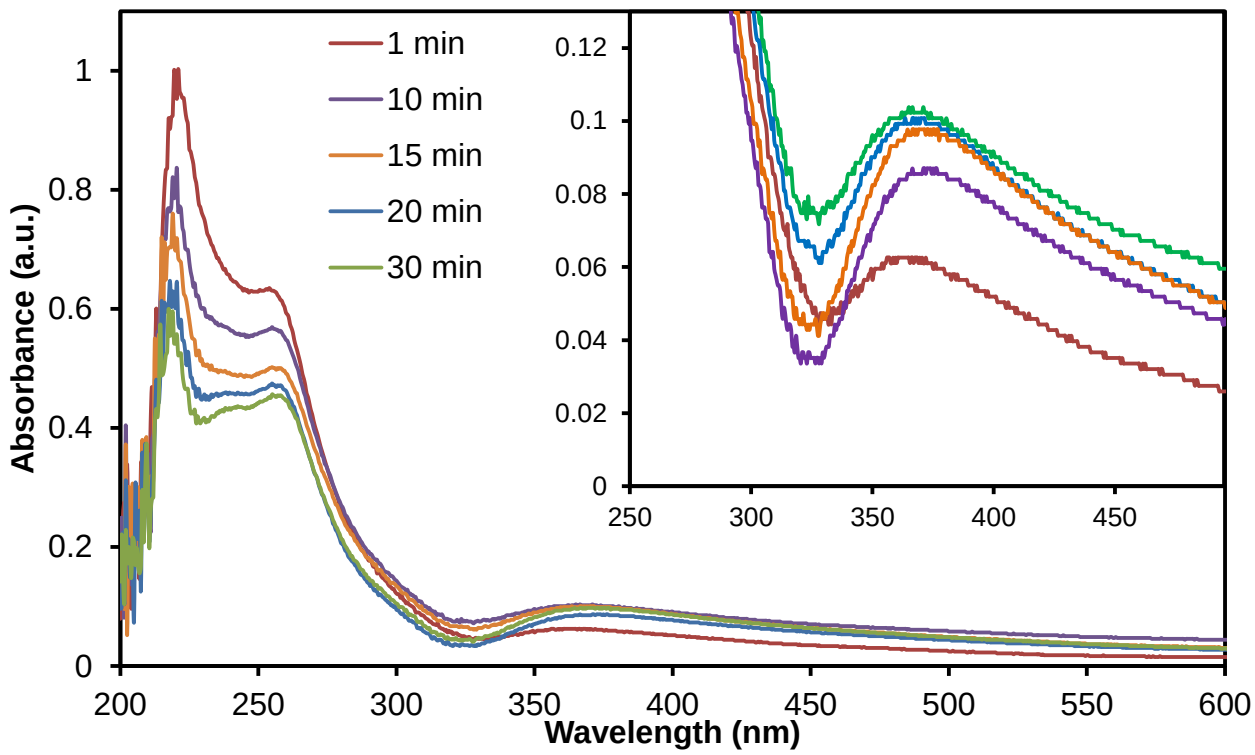

Figure 4: UV-Vis spectrophotometric analysis of synthesized AgNPs at pH 4.0

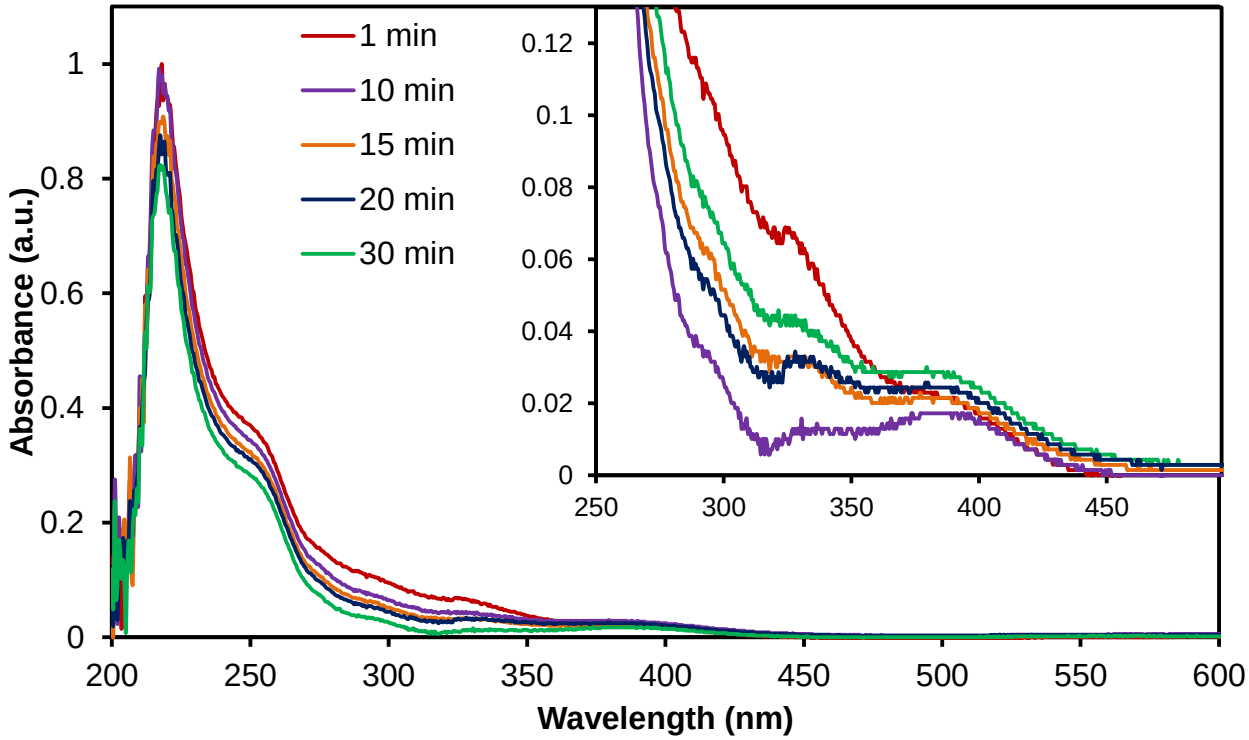

Figure 5:UV-Vis spectrophotometric analysis of synthesized AgNPs at pH 6.0

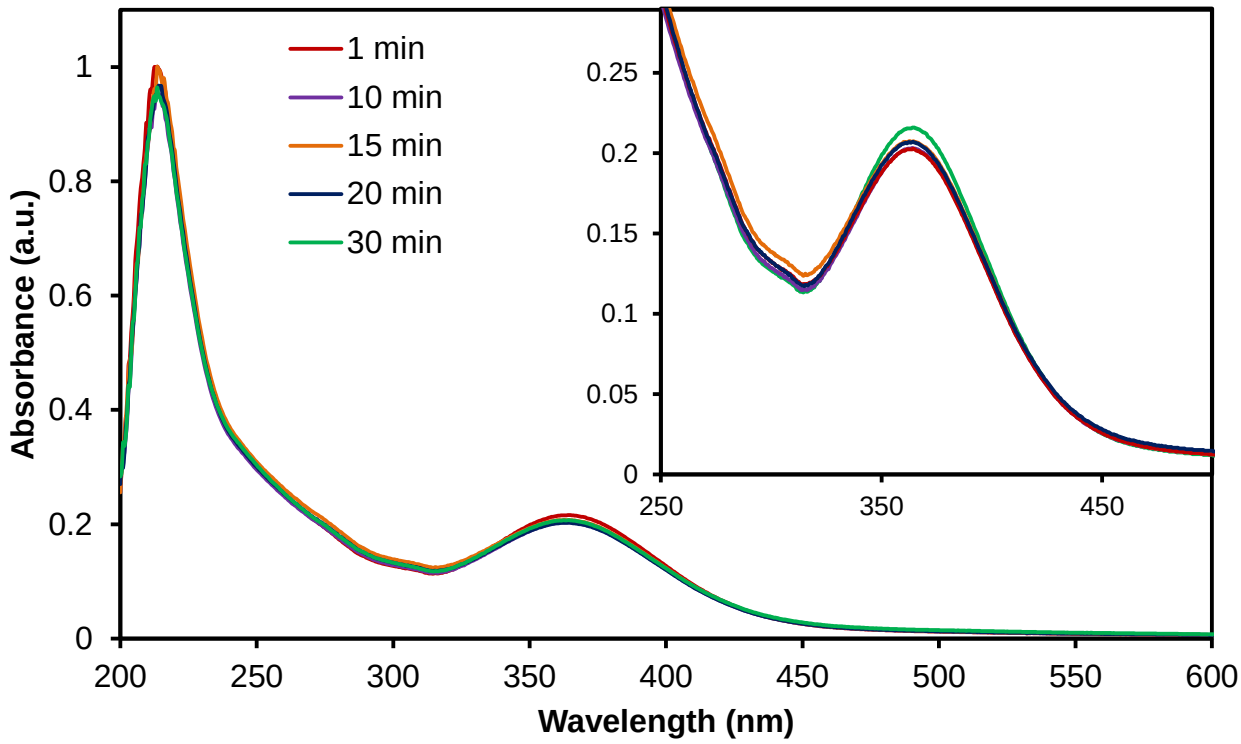

Figure 6:UV-Vis spectrophotometric analysis of synthesized AgNPs at pH 8.0

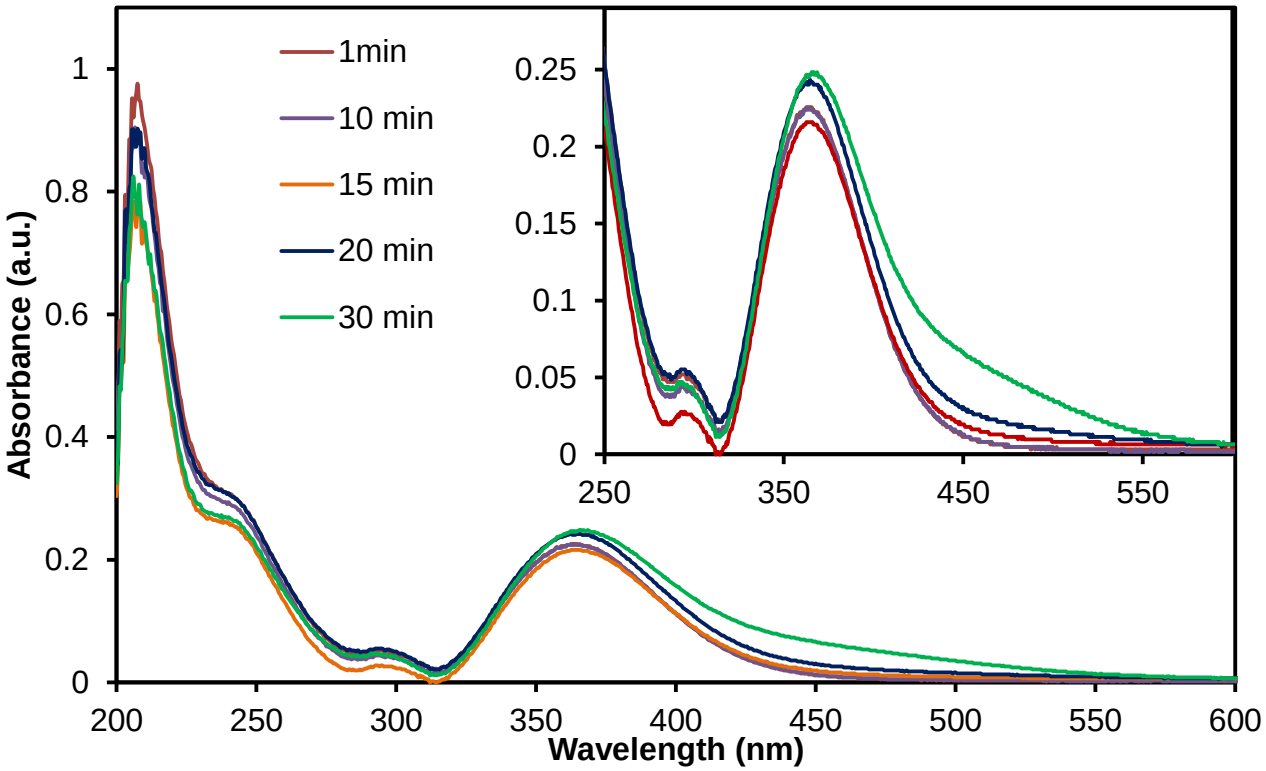

Figure 7: UV-Vis spectrophotometric analysis of synthesized AgNPs at pH 10.0

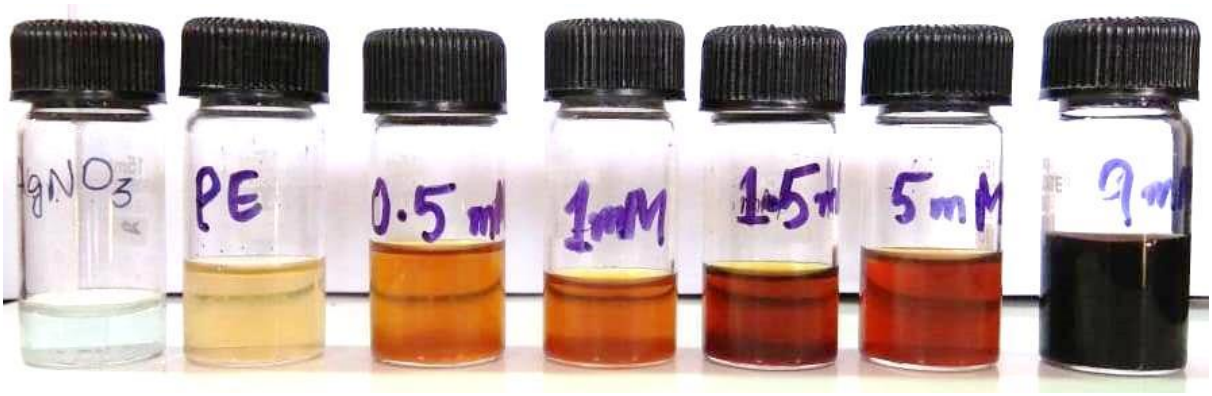

Figure 8: From left to right;$AgNO_3$solution, Pineapple peel extract,$AgNO_3$(0.5, 1, 1.5, 5, 9 mM) and peel extract mixture.

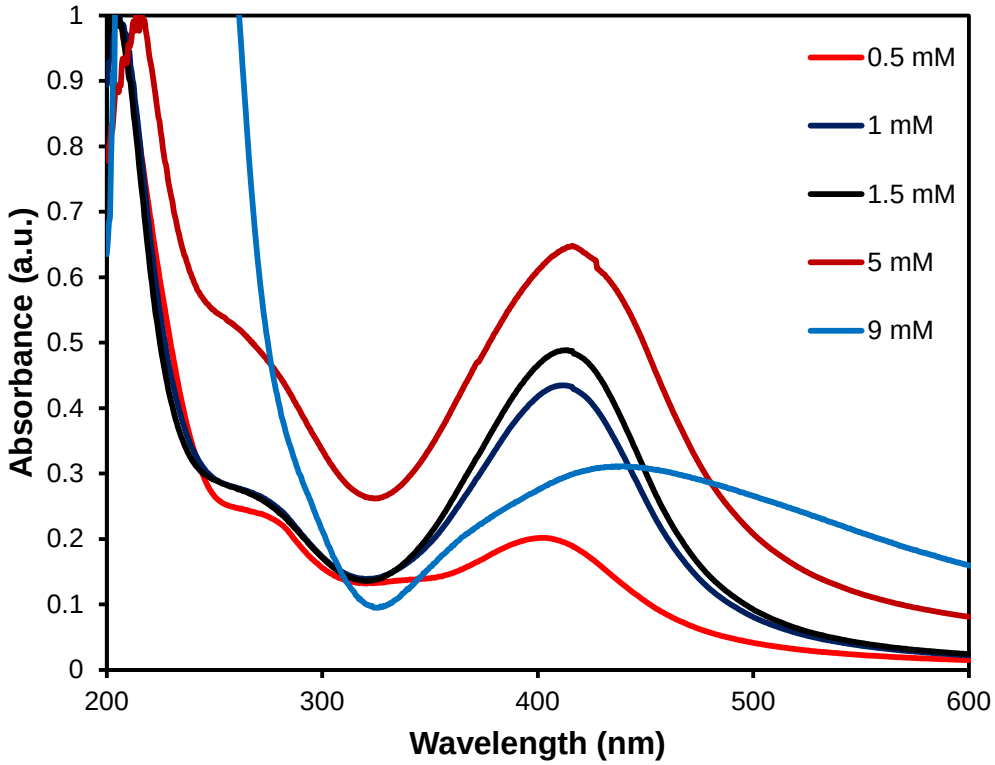

Figure 9:UV- Vis spectra of synthesized AgNPs with different concentrations.

The color of solution also gets dark with increase in time with increase in the final concentration of $AgNO_3$as shown in the figure 8. Figure 9 represents the, UV- Vis spectra of biogenic Ag NPs of different concentrations; absorbance peak for 0.5 mM, 1 mM, 1.5 mM, 5 mM, and 9 mM was observed at 400.5, 411, 414, 416, and 436 respectively.The red shift in

the peak with an increase in the final concentration of Ag represents that Ag concentration is directly proportional to the wavelength, but inversely proportional to the energy of particles. Hence, more is the final concentration of Ag, more is the stability of AgNPs in the sample.

4.1.2 DLS Analysis

DLS analysis is done to define the hydrodynamic radii of synthesized AgNPs. The size distribution as depicted from the graph for the final concentration of 0.5 mM $AgNO_3$ is 31.8 nm, for 1 mM, 1.5 mM, 5 mM, and 9 mM it is 17.5 nm, 14.5 nm, 18.8 nm, and 42.2 nm.As the concentration is increasing the size of NPs decreases up to certain concentration after which size of AgNPs starts rising up. Higher concentration of $AgNO_3$ in the reaction sample reduced to AgNPs by the compounds of plant extract. But when the concentration of $AgNO_3$ is lower then there is an aggregation of silver nanoclusters, which results in the NPs of larger diameter. Same happens when the concentration of $AgNO_3$is higher than certain range.

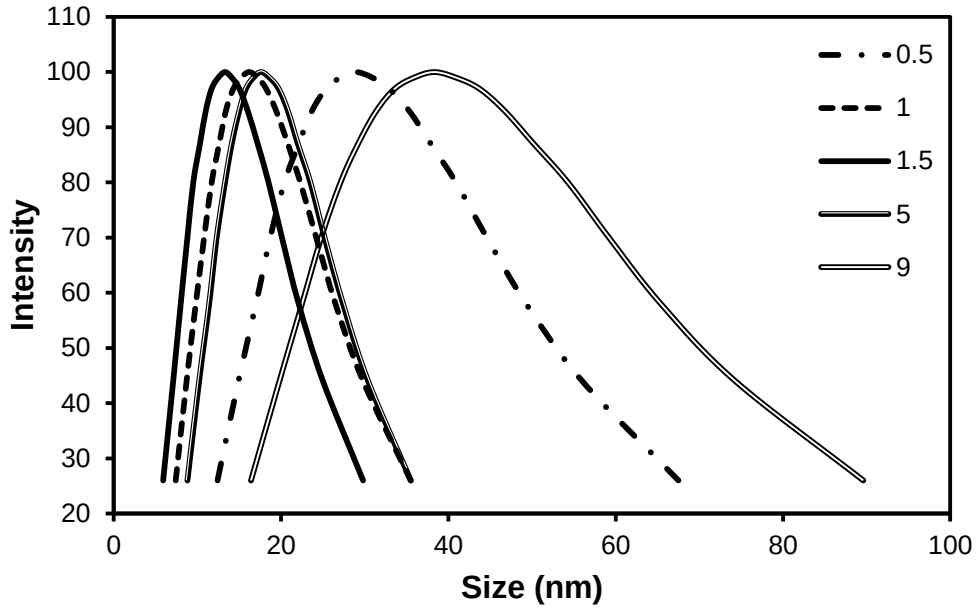

Figure 10: DLS analysis showing the size distribution of different concentrations of AgNPs synthesized.

4.1.3 FT-IR Analysis

FTIR spectroscopy is basically used to identify the compounds present in the sample, and its IR range is 400-4000 cm^{-1}. There is strongest peak observed at 3277 cm^{-1}, which indicated the O-H stretching and the peaks at 1638 cm^{-1} indicates the C=O stretching vibrations, and

this concludes the existence of carbonyl groups in the ethanolic content in plant extract. The peaks at 1600- 800 cm^{-1}represents the C=O stretching (lipids) and the peaks between 1600-720 cm^{-1}shows the presence of amide I band region. Further 1638 cm^{-1} peak corresponds to CO^{2-} stretching. Further peaks of other stretchings were also depicted from the graph, which includes N=O stretching, CH_3 stretching, O-N=O bending, C=C stretching, and all these indicates the presence of alkenes, amino acids, nitrites, nitrates, esters, ethers, alkynes, aldehydes, organic halogen, aromatic compounds and carbohydrates in the plant extract. No absorbance peak observed within the range of 2220-2260 cm^{-1} which specifies that there is no cyanide group present in the plant material. Peaks same as plant extracts were observed in the Ag NPs solution, this indicates that those functional groups are acting as capping agents to prevent further clustering of silver nanoparticles. Additional peaks in Ag NPs solution are of double and triple bonds of alkenes and alkynes as shown in figure 11.

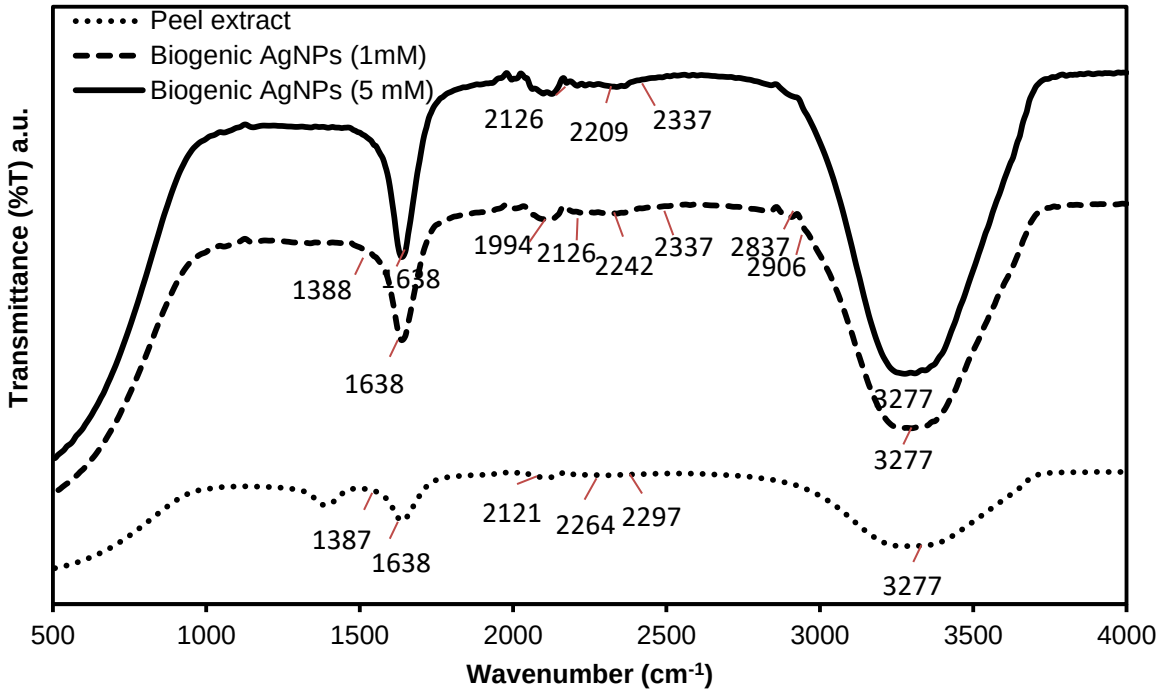

Figure 11: FT-IR analysis of peel extract and biogenically synthesized Ag NPs.

4.2 Standard curve of Mthylene Blue

Standard curve for methylene blue was prepared and the solutions were made with different concentration i.e. 0.1, 0.5, 1, 2, 5, 10, 15, 20, 25, 30, and 40 ppm. Absorbance was taken at 664 nm.

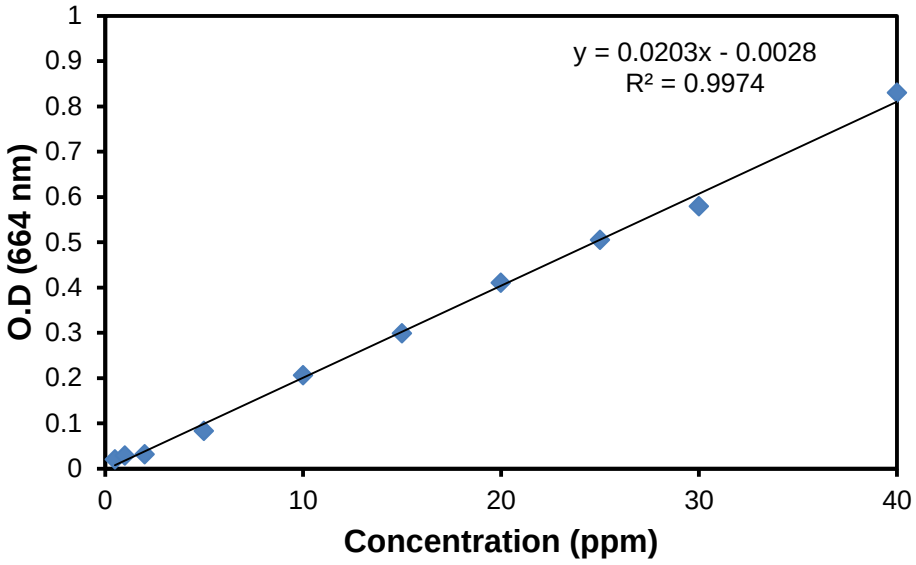

Figure 12: Standard curve of methylene blue

4.3 Dye Decolorization

Mechanism of decolorization of dye by silver nanoparticles leads to the shift of the valence band (VB) electrons to the conduction band (CB), which generates the positive holes and the free electrons. A water and oxygen molecule reacts with these free electrons and forms the free radicals as the products. These free radicals then directly oxidized the MB dye and leads to its decolorization (Sinha, et al 2016).

$$Ag\ (NPs) + Sunlight \longrightarrow Ag\ (e^-_{cb} + h_{vb}^+)$$

$$Ag\ (h_{vb}^+) + H_2O \longrightarrow Ag + H^+ + OH^-$$

$$Ag\ (e^-_{cb}) + O_2 \longrightarrow Ag + O_2{\cdot}^-$$

$$Ag\ (h_{vb}^+) + OH^- \longrightarrow Ag + OH{\cdot}$$

$$MB + OH{\cdot} \longrightarrow Oxidation\ products$$

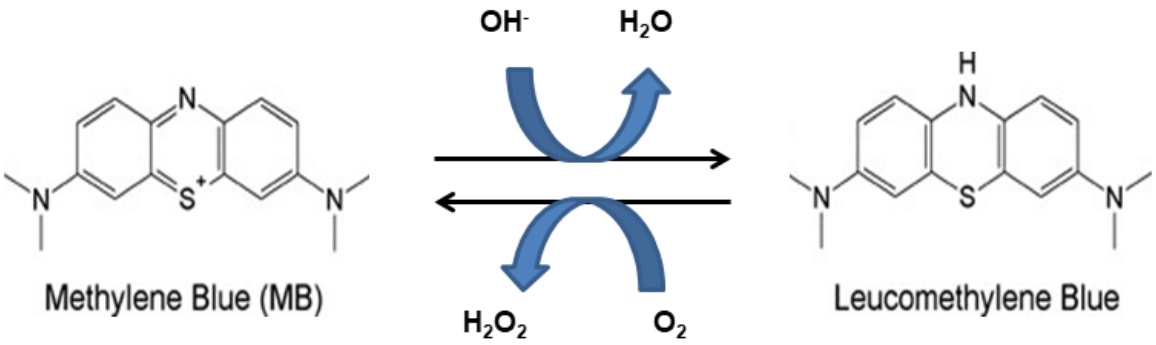

Figure 13: Mechanism for decolorization of MB dye by AgNPs

4.4 RSM

Single factor study

Various factors can effect the decolorization of dye, some of the experiments performed to check the effect of those factors. These include, a) effect of pH, b) effect of initial dye concentration (ppm), c) effect of AgNPs concentration (mM), and d) effect of time (min). Graphs are plotted as shown in figure 11. It was concluded, as the pH rises, decolorization (%) of dye also increses. The relation between dye concentration and the decolorization % is inversely proportional and with time it is directly proportional. The relation between dye decolorization and AgNPs concentration is not well co-related as the maximum decolorization was observed in the case of 1 mM and least in the case of 9 mM. Hence, only three factors considered in the RSM methodology, as mentioned below.

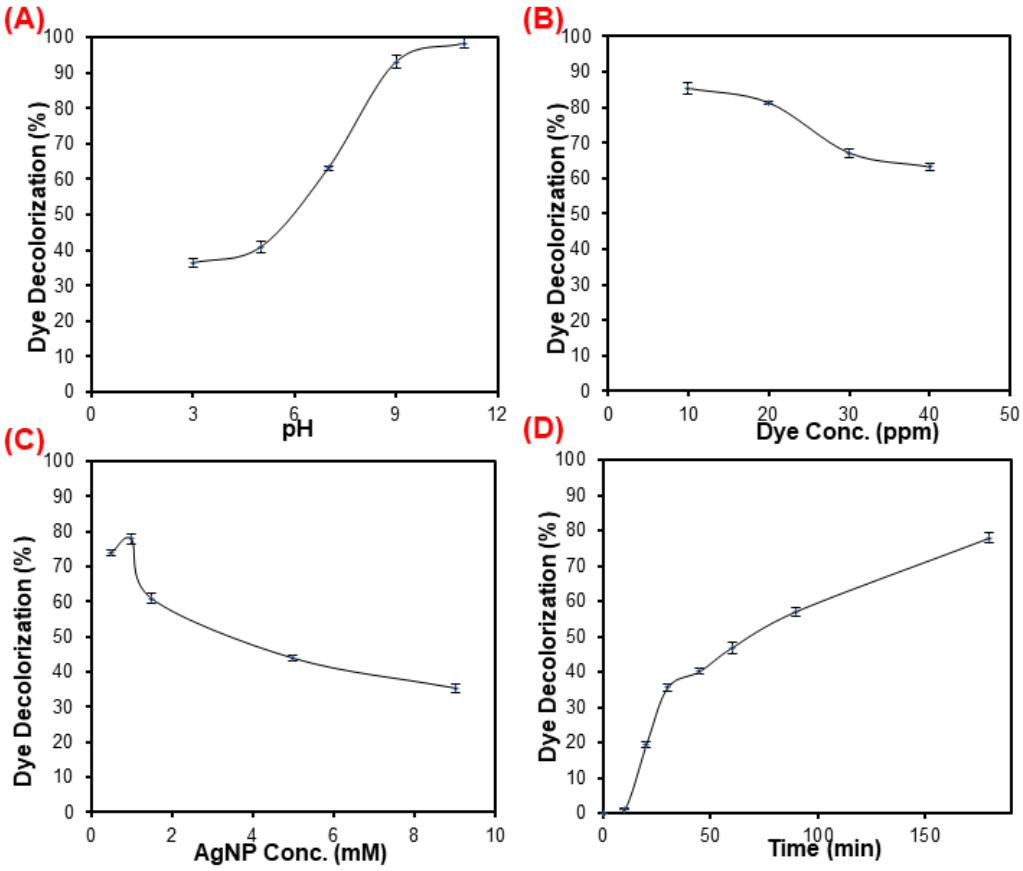

Figure 14: Effect of (A) pH, (B) Dye concentration (ppm), (C) AgNP concentration (mM), and (D) Time, on decolorization of methylene blue dye.

Model fitting Statistical analysis

Detailed results of the experiment for dye decolorization by biogenically synthesized silver nanoparticles are listed in Table 2 as actual and predicted dye decolorization (%).The polynomial coefficients for every term of the equation was determined by analysis of multiple regression using the design expert 6.0.8. The absolute equation in terms of the actual factors with significant terms, which affects the enzyme loading onto D-MHNTs are represented as follows:

$$\text{Decolorization (\%)} = 29.66173+4.80716A-2.82514B+0.35554C-0.13190A^2+0.017261B^2 -1.62634E\text{-}003C^2+0.15548AB+0.022409AC+1.03588E\text{-}003BC$$

Where, A is the pH of the solution; B is dye concentration (ppm); and C is Time (min).

Table 7:RSM based Box-Behnekn experimental design for the independent variables and their corresponding response (Dye Decolorization (%)) for MB decolorization by Ag NPs

Run	pH	Dye Conc. (ppm)	Time (min)	Dye Decolorization (%)	
				Actual	Predicted
1	7.00	10.00	180.00	**85.42**	**82.61**
2	10.00	40.00	95.00	**88.33**	**85.67**
3	10.00	25.00	180.00	**96.51**	**99.87**
4	7.00	25.00	95.00	**59.44**	**60.68**
5	7.00	25.00	95.00	**58.48**	**60.68**
6	4.00	25.00	10.00	**10.39**	**7.04**
7	4.00	40.00	95.00	**17.27**	**17.82**
8	7.00	25.00	95.00	**60.60**	**60.68**
9	7.00	10.00	10.00	**45.57**	**46.27**
10	7.00	40.00	180.00	**62.69**	**61.99**
11	4.00	10.00	95.00	**52.40**	**55.07**
12	10.00	25.00	10.00	**49.61**	**49.46**
13	4.00	25.00	180.00	**34.43**	**34.59**
14	7.00	40.00	10.00	**17.55**	**2037**
15	10.00	10.00	95.00	**95.48**	**94.94**
16	7.00	25.00	95.00	**62.71**	**60.68**
17	7.00	25.00	95.00	**62.13**	**60.68**

Model Validation

The competence of the generated exemplary was interpreted by variance analysis.The ANOVA results for the generated model is shown in Table 8. The lack of fit (variation of dataaround the fitted model) was evaluated by employing the F-test.The F-testassociates thetreatment variance and error variance.Lack of Fit F-valueof 5.73 infers that thesevalues are irrelevant at a 95% level of significance.The F-value of the model (126.65) with a p-value lessthan 0.0001 represents that the generated model was significant at the 95% confidence level.A low p-value obtained signifies that the model generated is in good harmony with the

response observed. It also confirms that the change in response is due to a real cause, i.e. change in the independent variables, not by any kind of error or noise.

Table 8:ANOVA results for coefficients of response surface quadratic model

Source	Sum of Square	DF	Mean Square	F Value	Prob>F	Remarks
Model	10893.15	9	1210.35	126.65	< 0.0001	significant
A	5801.26	1	5801.26	607.02	< 0.0001	
B	1082.09	1	1082.09	113.23	< 0.0001	
C	3038.89	1	3038.89	317.98	< 0.0001	
A^2	5.93	1	5.93	0.62	0.4566	
B^2	63.51	1	63.51	6.65	0.0366	
C^2	581.34	1	581.34	60.83	0.0001	
AB	195.80	1	195.80	20.49	0.0027	
AC	130.61	1	130.61	13.67	0.0077	
BC	6.98	1	6.98	0.73	0.4211	
Residual	66.90	7	9.56			
Lack of Fit	54.27	3	18.09	5.73	0.0624	not significant
Pure Error	12.63	4	3.16			
Cor Total	10960.05	16				

The importance of each varible in the model was inspected by testing the null hypothesis, as shown in table 8. According to ANOVA, the linear term of pH of the solution (A) has the greatest effect on dye decolorization (%) due to the large F-value of 607.02. On the other hand, Initial dye concentration (B) also seems to have a significant result on the dye decolorization (%), along with the quadratic term (B^2) has a significant effect owing to their F-values of 113.23 and 6.65 respectively.Time of irradiation (C) also shows a substantial effect to the response as well as the quadratic term (C^2), and the interactions between the independent variables(AB,AC).

The R^2value as shown in table 9, was establish to be 0.9939, that is close to 1, whichindicates a great correlation between predictedandexperimental values. Itshows that 99.39 % variabilityresponse for dye decolorization (%) isspecified by the model thus, only about 0.61%, data dissimilarity for the corresponding response is not elucidated by the model.Adjusted R^2 (Adj-R^2) is more suitable in a system with various number of independent variables, for evaluating the model goodness.The values of Adj-R^2 and Pre-R^2 were also in reasonable agreement (0.9860 and 0.9190) i.e. the variance is less than 0.2.Acceptable precision measures the ratio of signal to noise, a ratio better than 4 is anticipated for an acceptable model, in our case it was obtained to be 39.155, thus indicating that this model is useful to navigate the design space.

Table 9:ANOVA results of response surface quadratic model

Std. Dev.	3.09	**R-Squared**	0.9939
Mean	56.42	**Adj R-Squared**	0.9860
C.V.	5.48	**Pred R-Squared**	0.9190
PRESS	888.05	**Adeq Precision**	39.155

Effect of variables

Furthermore, the model suitability can be confirmed by investigation of the residuals (difference between the predicted and observed response). The predicted values of dye decolorization are plotted versus corresponding observed values as shown in Fig 14. It can be observed easily that the residuals are in the vicinity of the straight line. Hence, the generated model is considered to be acceptable.

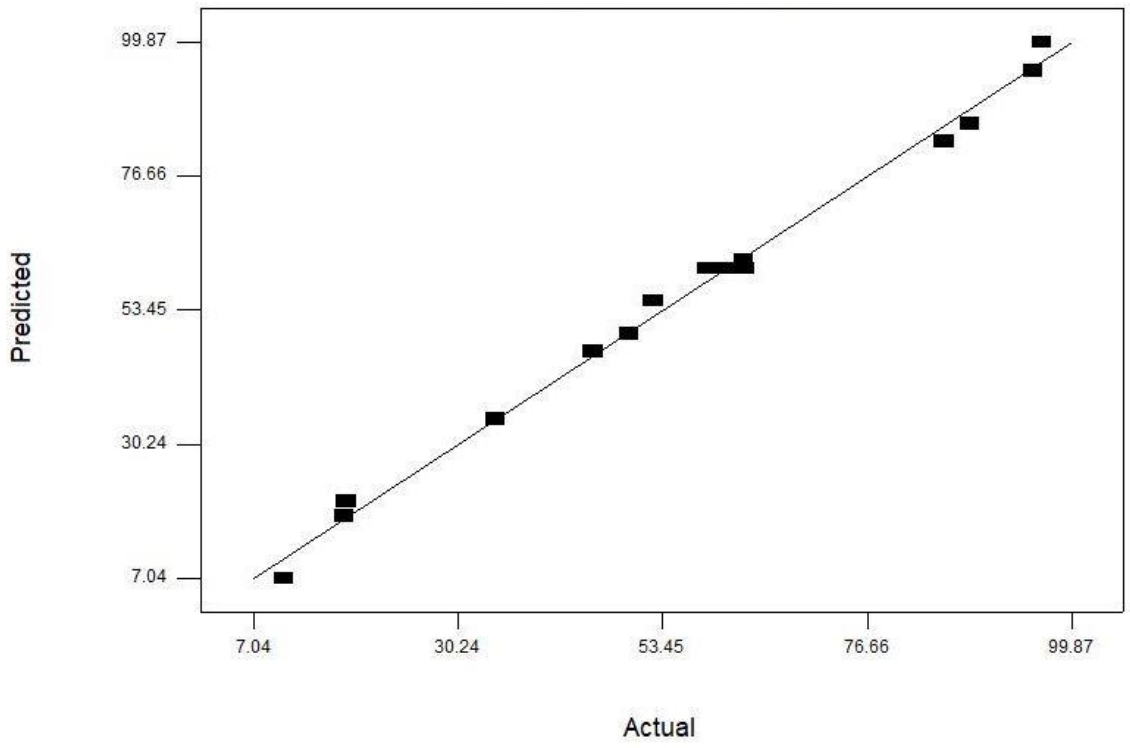

Figure 15: Comparison of the experimental results of dye decolorization with the predicted values.

The individual effect of the independent variables, on the MB dye decolorization (%), was examined by perturbation plots. This plots is functional to examine the most substantial factors on the response. It utilizes the model terms to show the consequence of each variable that deviate from the center point (midpoint or coded value 0) on the response. A steep curvature or slope is the indication that the response is subtle to that particular variable. While, a straight line specifies that response is insensitive to the variation in that variable. Perturbation plots for the MB dye decolorization are represented in Fig 15. The pH (A) curve shows an inclined line indicating that this factor had maximum and direct effect on the response as the dye decolorization increases steeply as the pH is moving towards alkaline. On the other side, the steep curvatures in initial dye concentration (B) and irradiation time (C) curves specify that the dye decolorization was subtle to these variables. When the initial dye concentration is increased the dye decolorization decreases accordingly. Furthermore, the dye decolorization significantly increases as the irradiation time is moved towards the high value.

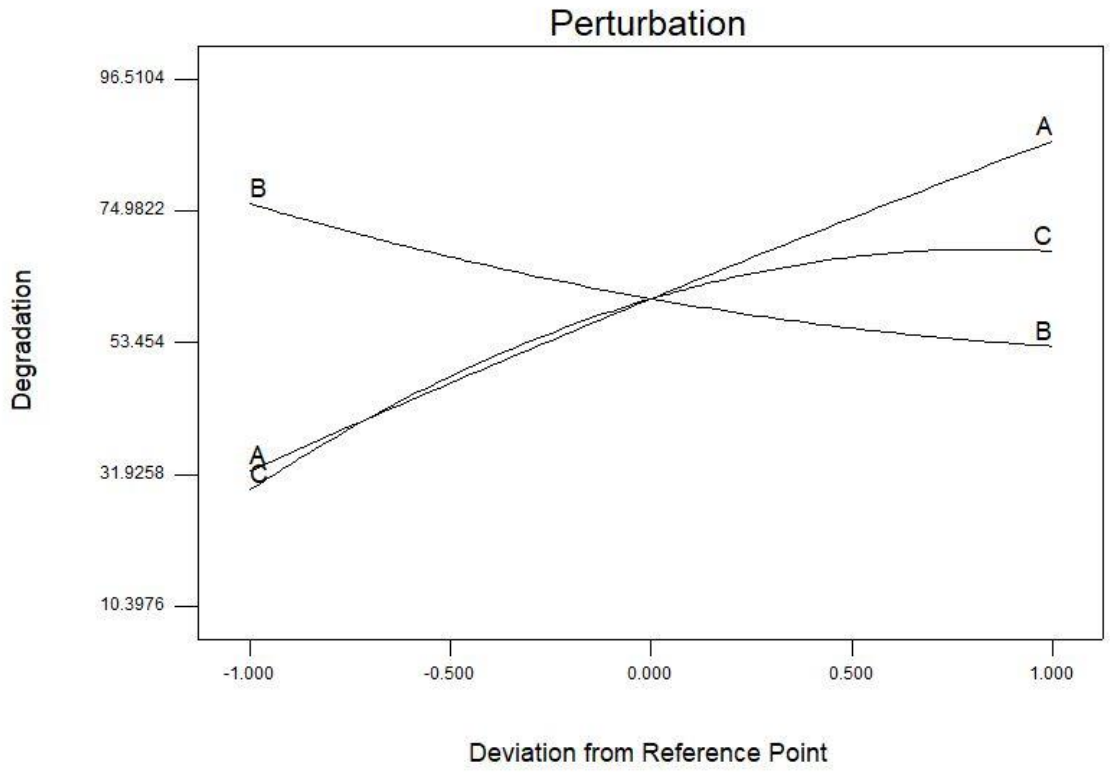

Figure 16: Perturbation plots for the dye decolorizationof MB. A, pH; B, dye concentration; and C is irradiation time.

To perceive the shape of response3-D surfaces and delineations were plotted by keeping the one variable constant and the other 2 variables varying within the experimental ranges.

As can be seen in Fig 16, the combined effect of pH and initial concentration of MB on the rate of its decolorization is plotted at the constant irradiation time 95 min. The decolorization increases with moving pH values towards an alkaline environment as compared with acidic or neutral environment. While at a particular pH if the initial dye concentration was increased a decline was observed in the decolorization.

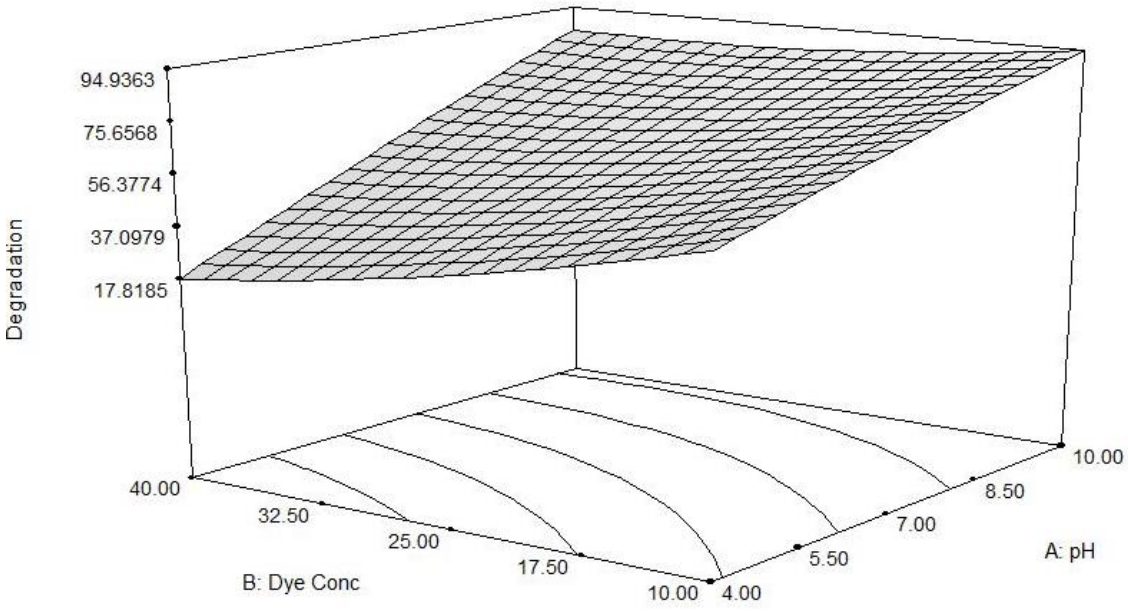

Figure 17: The response 3-D surface plot of the dye decolorization as the function of pH and Dye concentration (Irradiation time =95 min).

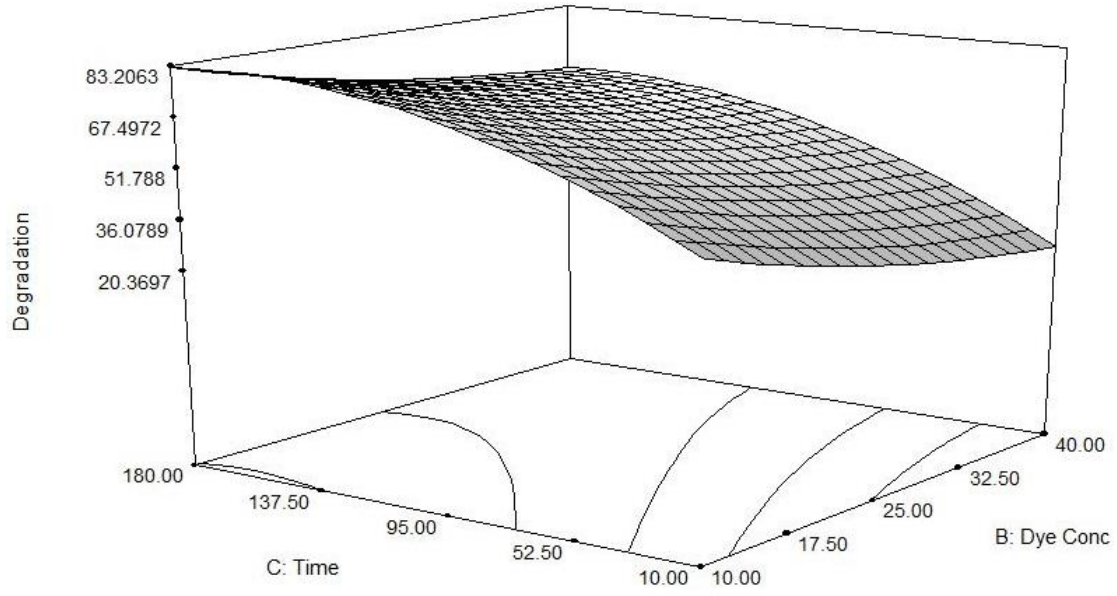

Figure 18: The response 3-D surface plot ofthe dye decolorization as the function of Dye concentration and irradiation time (pH =7).

It was found from plotting surface response and counter plot between pH and irradiation time at a constant dye concentration (25 ppm) that the MB dye decolorization was significantly altered by change in both irradiation time and pH. Dye decolorization increases

with increase in irradiation time as the fact that first the dye particles are adsorbed on the catalyst surface and then the photocatalysis reaction takes place.In fact, larger exposure means more production of hydroxyl radicals, which are accountable for oxidizing the MB dye molecules. While for pH, it was also confirmed from Fig. 17 that the dye decolorization considerably increased with increasing pH.

Optimization of MB Decolorization

The main aim of this research study was to discover the optimum values of operational parameters that will produce maximum dye decolorization. The present study, the process was optimized under three constraints. First is the pH of the reaction solution was in range, second is the minimization of the irradiation time and the third is maximization of the initial concentration of MB. With Design expert Version 6.0.8, numerical optimization was carried out by taking three independent variables and the dye decolorization as responses. To confirm the model suitability the optimization condition obtained from the model was verified by conducting experiments under the prophesied optimal conditions as shown in Table 10. The harmony between the observed and the predicted values confirmed the legitimacy of the generated model for stimulating the dye decolorization by biologically synthesized silver nanoparticles.Experiments were conducted in triplicates and the average values are stated.

Table 10: Obtained optimum values of the process variables and response

Variable	Value	Dye decolorization (%)	
		Predicted	Experimental
pH	9.96		
Dye concentration (ppm)	40	99.9	98.04±0.23
Time (min)	173.22		

Optimized condition that is deduced from the RSM methodology was reaction mixture with 9.96 pH, with decolorization of 40 ppm dye after 173.22 min. The UV- Vis spectrum from range 200- 800 nm was taken and it is shown in the graph below.

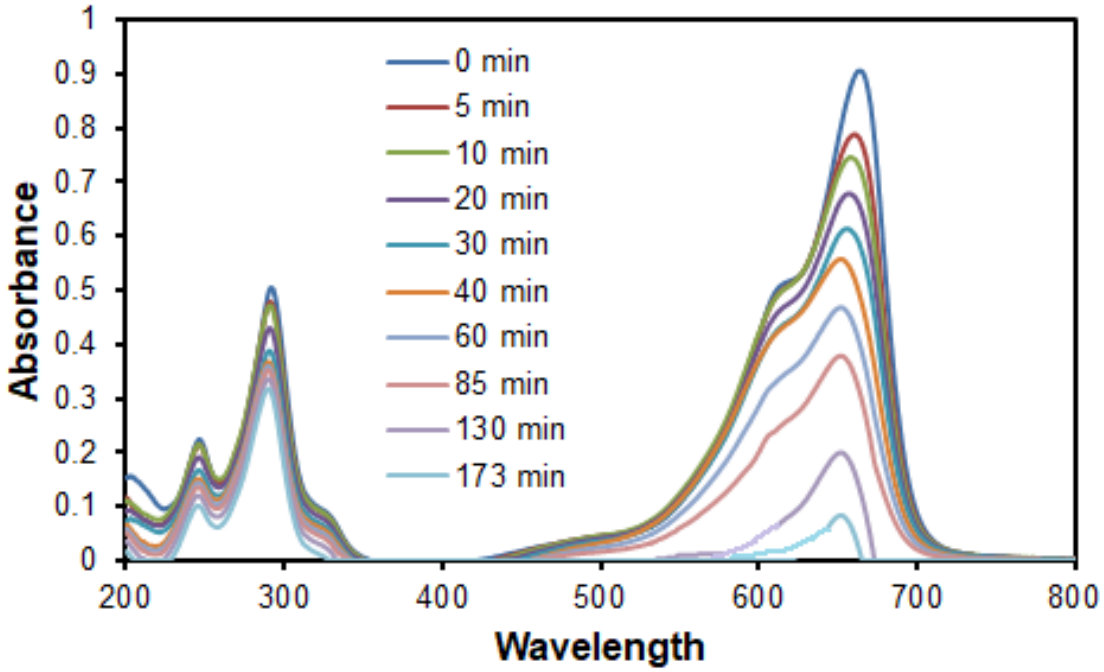

Figure 19: Decolorization of MB dye with optimized conditions.

4.5 Kinetic modelling of photocatalytic decolorization of MB dye

Kinetic models are tool that contributes to the design for photocatalytic decolorization of dye in wastewater at pilot or full-scale (Lin, 2014). To understand the decolorization of dye, and its mechanism, four types of kinetic modeling were done (first-order, pseudo first-order, second-order, and pseudo second-order; figure 15). The value of coefficient R^2 is also mentioned in the figure. From the figure 19; it was concluded that the kinetics of MB dye decolorization by AgNPs follows the model of pseudo second-order, as the value of R^2 is closer to the value of 1 in this model. Photocatalytic decolorization follows the first order, second order and pseudo second order kinetics. First-order kinetics illustrate that the rate of reaction is proportional to the substrate. Whereas, second-order specifies that rate of reaction is directly related to the two types of substrates; and pseudo second-order kinetics specify that the step of monolayer sorption by photo induced electron transfer between dye molecules and the photocatalyst is the rate-limiting step (Hu et al., 2013).

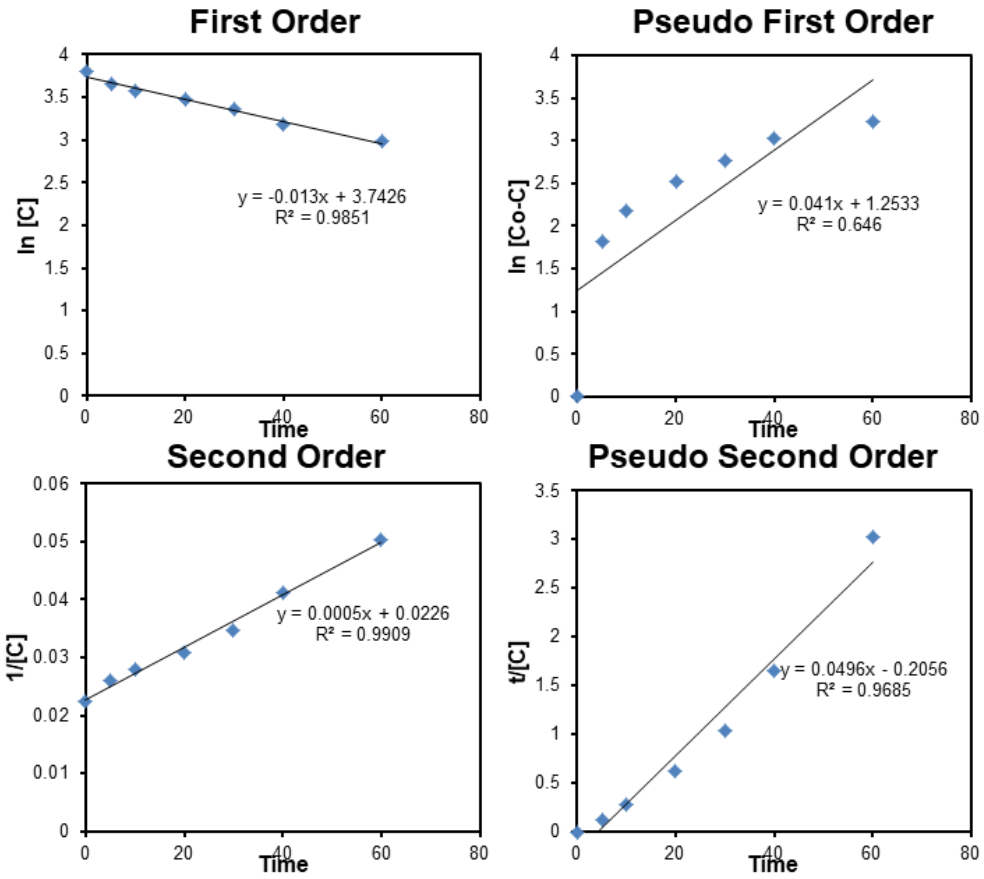

Figure 20: Kinetic model of photocatalytic decolorization of MB by AgNPs.

4.6 Antibacterial Activity

Biogenic Ag NPs shows noticeable bactericidal activity against *Pseudomonas aeruginosa* (gram-negative) and *Bacillus subtilis* (gram-positive). Ag NPs with 1 mM concentration shows a prominent zone of inhibition with average size of 6 mm radii, as shown in figure 21. The anti-bacterial property of biogenic Ag NPs is basically because of silver cations (Ag^{+2}). These silver cations due to electrostatic attraction binds with cell wall of bacteria and penetrates inside the cell, therefore, disrupts the cell mechanism by attacking its DNA and other organelles (Ajitha et al., 2018).

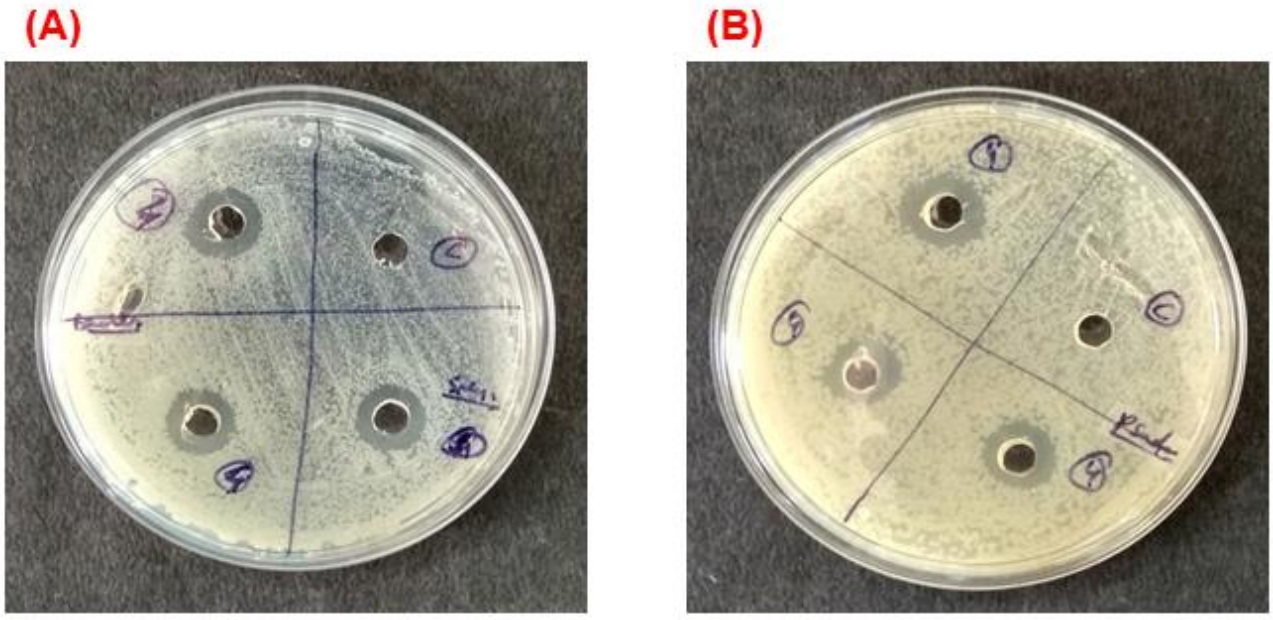

Figure 21: Zone of inhibition of Ag NPs (1 mM) in (A) *Bacillus subtilis*, (B) *Pseudomonas aeruginosa*

CONCLUSION

Biogenic synthesis of silver nanoparticles has developed as better and simple preference than chemical and physical methods as it is easy, fast, cost-effective as well as eco-friendly substitute. In the recent study, AgNPs were synthesized from the pineapple peel waste extract (*Ananas comosus*) within 10 min of reaction time. Biosynthesized AgNPs has an average diameter of 25 nm. Functional groups were analyzed by the FT-IR which contributes to reduction and capping of AgNPs during the reaction period. The investigation over photocatalysis concludes that AgNPs have an efficient effect on MB decolorization under direct sunlight and can be applicable in waste water treatment plants and also in different industries. Also, biogenically synthesized Ag NPs are showing excellent antimicrobial efficacy and therefore, have potential utilization in the field of biomedical sciences.

REFERENCES

- Ahmed, S., Ahmad, M., Swami, B. and Ikram, S. (2015). A review on plants extract mediated synthesis of silver nanoparticles for antimicrobial applications: A green expertise.*Journal of Radiation Research and Applied Sciences*,pp. 589-596.
- Amendola, V. and Meneghetti, M. (2009). Size evaluation of gold nanoparticles by UV−vis spectroscopy. *The Journal of Physical Chemistry C*, 113(11), pp.4277-4285.
- Ameta, R., Benjamin, S., Ameta, A. and Ameta, S. (2012). Photocatalytic degradation of organic pollutants: A review. *Materials Science Forum*, 734, pp.247-272.
- Anandalakshmi, K., Venugobal, J. and Ramasamy, V. (2015). Characterization of silver nanoparticles by green synthesis method using *Pedalium murex* leaf extract and their antibacterial activity. *Applied Nanoscience*, 6(3), pp.399-408.
- Anon, (2017). Green synthesis of silver nanoparticles from *Leea indica*and its applications. *International Journal of Pharmaceutical Sciences and Research*, 8(3), pp. 232-246.
- Anjum, D. (2016). Characterization of nanomaterials with transmission electron microscopy. *IOP Conference Series: Materials Science and Engineering*, 146, pp.012001.
- Bauer, M. and Schnapp, G. (2012). Protein production for three-dimensional structural analysis. *Reference Module in Chemistry, Molecular Sciences and Chemical Engineering*, pp. 962- 975.
- Bar, H., Bhui, D., Sahoo, G., Sarkar, P., De, S. and Misra, A. (2009). Green synthesis of silver nanoparticles using latex of *Jatropha curcas*. *Colloids and Surfaces A: Physicochemical and Engineering Aspects*, 339(1-3), pp.134-139.
- Bensalah, N., Alfaro, M. and Martínez-Huitle, C. (2009). Electrochemical treatment of synthetic wastewaters containing alphazurine azo dye. *Chemical Engineering Journal*, 149(1-3), pp.348-352.
- Beydoun, D., Amal, R., Low, G. and McEvoy, S. (1999). Role of nanoparticles in photocatalysis.*Journal of Nanoparticle Research*, pp.439-458.
- Bhushan, B. (n.d.). *Springer handbook of nanotechnology*, pp. 467-469.

- Chen, D. (1999). Photocatalytic kinetics of phenol and its derivatives over UV irradiated TiO_2. *Applied Catalysis B: Environmental*, 23(2-3), pp.143-157.
- Chowdhury, A., Kunjiappan, S., Bhattacharjee, C., Somasundaram, B. and Panneerselvam, T. (2017). Biogenic synthesis of *Marsilea quadrifolia* gold nanoparticles: a study of improved glucose utilization efficiency on 3T3-L1 adipocytes. *In Vitro Cellular & Developmental Biology - Animal*, 53(6), pp.483-493.
- Faisal M, Tariq MA, Muneer M (2007) Photocatalysed degradation of two selected dyes in UV-irradiated aqueous suspensions of titania. *Dyes Pigments* 72: pp. 233–239.
- Lakshmanan, G., Sathiyaseelan, A., Kalaichelvan, P.T., Murugesan, K. (2018). Plant-mediated synthesis of silver nanoparticles using fruit extract of *Cleome viscosa* L.: Assessment of their antibacterial and anticancer activity. *Karbala International Journal of Modern Science*, 4(1), pp.61-68.
- Gavade, N., Kadam, A., Suwarnkar, M., Ghodake, V. and Garadkar, K. (2015). Biogenic synthesis of multi-applicative silver nanoparticles by using *Ziziphus Jujuba* leaf extract. *Spectrochimica Acta Part A: Molecular and Biomolecular Spectroscopy*, 136, pp.953-960.
- Gharibshahi, L., Saion, E., Gharibshahi, E., Shaari, A. and Matori, K. (2017). Structural and optical properties of Ag nanoparticles synthesized by thermal treatment method. *Materials*, 10(4), pp.402.
- Ghosh SK., Kundu S., Mandal M., Pal T. (2002) Silver and gold nanocluster catalyzed reduction of methylene blue by arsine in a micellar medium, *Langmuir*,18: pp. 8756–8760.
- Gorbe, M., Bhat, R., Aznar, E., Sancenón, F., Marcos, M., Herraiz, F., Prohens, J., Venkataraman, A. and Martínez-Máñez, R. (2016). Rapid biosynthesis of silver nanoparticles using pepino (*Solanum muricatum*) leaf extract and their cytotoxicity on HeLa cells. *Materials*, 9 (5), pp. 325.
- Hao, O., Kim, H. and Chiang, P. (2000). Decolorization of Wastewater. *Critical Reviews in Environmental Science and Technology*, 30(4), pp.449-505.

- Horie, M. and Fujita, K. (2011). Toxicity of Metal Oxides Nanoparticles. *Advances in Molecular Toxicology*, pp.145-178.
- Howe, J., Fultz, B. and Miao, S. (2012). Transmission Electron Microscopy. *Characterization of Materials*, pp. 361-365.
- Hsu, T. and Chiang, C. (1997). Activated sludge treatment of dispersed dye factory wastewater. *Journal of Environmental Science and Health . Part A: Environmental Science and Engineering and Toxicology*, 32(7), pp.1921-1932.
- Ibrahim, H. (2015). Green synthesis and characterization of silver nanoparticles using banana peel extract and their antimicrobial activity against representative microorganisms. *Journal of Radiation Research and Applied Sciences*, 8(3), pp.265-275.
- Iravani, S. and Zolfaghari, B. (2013). Green synthesis of silver nanoparticles using*Pinus eldarica*bark extract. *BioMed Research International*, 2013, pp.1-5.
- K. Jha, A. and Prasad, K. (2011). Green fruit of chili (*Capsicum annum L.*) synthesizes nano silver. *Digest Journal of Nanomaterials and Biostructures*, 6(no.4), pp.1717-1723.
- Kansal, S., Singh, M. and Sud, D. (2008). Studies on TiO_2/ZnO photocatalysed degradation of lignin. *Journal of Hazardous Materials*, 153(1-2), pp.412-417.
- Kumar, V. and Yadav, S. (2008). Plant-mediated synthesis of silver and gold nanoparticles and their applications.*Green Chemistry*, pp. 421-425
- Kumar, P., Govindaraju, M., Senthamilselvi, S. and Premkumar, K. (2013). Photocatalytic degradation of methyl orange dye using silver (Ag) nanoparticles synthesized from *Ulva lactuca*. *Colloids and Surfaces B: Biointerfaces*, 103, pp.658-661.
- Lingaraju, K., Raja Naika, H., Manjunath, K., Basavaraj, R., Nagabhushana, H., Nagaraju, G. and Suresh, D. (2015). Biogenic synthesis of zinc oxide nanoparticles using *Ruta graveolens* (L.) and their antibacterial and antioxidant activities. *Applied Nanoscience*, 6(5), pp.703-710.

- Logeswari, P., Silambarasan, S. and Abraham, J. (2015). Synthesis of silver nanoparticles using plants extract and analysis of their antimicrobial property. *Journal of Saudi Chemical Society*, 19(3), pp.311-317.
- Lu, G. and Gao, P. (2010). Emulsions and microemulsions for topical and transdermal drug delivery. *Handbook of Non-Invasive Drug Delivery Systems*, pp.59-94.
- Maes, K. and Willems, J. (2011). Photochemistry: UV/VIS spectroscopy, photochemical reactions and photosynthesis (Chemical engineering methods and technology). *New York: Nova Science Publishers*, pp. 98-106.
- Manikandan, V., Velmurugan, P., Jayanthi, P., Park, J., Chang, W., Park, Y., Cho, M. and Oh, B. (2017). Biogenic synthesis from *Prunus* × *yedoensis* leaf extract, characterization, and photocatalytic and antibacterial activity of TiO_2 nanoparticles. *Research on Chemical Intermediates*, 44(4), pp.2489-2502.
- Malik, A. and Grohmann, E. (2012). Environmental protection strategies for sustainable development. *Advance in Microbiology*, pp. 259-271.
- Mathur, N. (2006). Assessing mutagenicity of textile dyes from Pali (Rajasthan) using ames bioassay. *Applied Ecology and Environmental Research*, 4(1), pp.111-118.
- Mock, J., Barbic, M., Smith, D., Schultz, D. and Schultz, S. (2002). Shape effects in plasmon resonance of individual colloidal silver nanoparticles. *The Journal of Chemical Physics*, 116(15), pp.6755-6759.
- Mohanpuria, P., Rana, N. and Yadav, S. (2007). Biosynthesis of nanoparticles: technological concepts and future applications. *Journal of Nanoparticle Research* 10(3), pp. 507-517
- Murugan, K., Dinesh, D., Kumar, P., Panneerselvam, C., Subramaniam, J., Madhiyazhagan, P., Suresh, U., Nicoletti, M., Alarfaj, A., Munusamy, M., Higuchi, A., Mehlhorn, H. and Benelli, G. (2015). Datura metel-synthesized silver nanoparticles magnify predation of dragonfly nymphs against the malaria vector Anopheles stephensi. *Parasitology Research*, 114(12), pp.4645-4654.

- Pagga, U. (1994). Development of a method for adsorption of dyestuffs on activated sludge. *Water Research*, 28(5), pp.1051-1057.

- Palanisamy, k., kalaiselvi1, p., gabriel, m., thangavel, j. And sundaram, l. (2014). *Emblica officinalis* leaf extract mediated green synthesis of antibacterial silver nanoparticles against human pathogens. *World Journal of Pharmacy and Pharmaceutical Sciences*, 3(3), pp. 4261-4270.

- Pandian, M. (2014). X-ray diffraction analysis: principle, instrument and applications. *Dataset* March, pp. 103-112.

- Pareek, N., Dhaliwal, A. and Malik, C. (2012). Biogenic synthesis of silver nanoparticles, using *Bougainvillea spectabilis* wild. bract extract. *National Academy Science Letters,* 35(5), pp.383-388.

- Rokhade, V. and Taranath, T. (2017). Photosynthesis of silver nanoparticles using fruit extract of *Leea indica (burm. f) merr*. and their antimicrobial activity. *International Journal of Pharmaceutical Sciences and Research*, 8(3), pp. 465-470.

- Sinha, T., Ahmaruzzaman, M. and Bhattacharjee, A. (2016). A green and facile synthesis of silver nanoparticles and it's applications in the reduction and photodegradation of organic compounds. *Indian Journal of Chemical Technology*, 23, pp. 462-468.

- Sobana N., Muruganadham M., Swaminathan M. (2006) Nano-Ag particles doped TiO_2 for efficient photodegradation of direct azo dyes. *Journal of Molecular Catalysis* A 258: pp. 124–132.

- Tan, I., Hameed, B. and Ahmad, A. (2007). Equilibrium and kinetic studies on basic dye adsorption by oil palm fibre activated carbon. *Chemical Engineering Journal*, 127(1-3), pp.111-119.

- Trenerry, V. and Rochfort, S. (2012). Natural Products Research and Metabolomics. *Reference Module in Chemistry, Molecular Sciences and Chemical Engineering*, pp. 123-131.

- Veerasamy, R., Xin, T., Gunasagaran, S., Xiang, T., Yang, E., Jeyakumar, N. and Dhanaraj, S. (2011). Biosynthesis of silver nanoparticles using mangosteen leaf extract and evaluation of their antimicrobial activities. *Journal of Saudi Chemical Society*, 15(2), pp.113-120.
- Veisi, H., Azizi, S. and Mohammadi, P. (2018). Green synthesis of the silver nanoparticles mediated by *Thymbra spicata* extract and its application as a heterogeneous and recyclable nanocatalyst for catalytic reduction of a variety of dyes in water. *Journal of Cleaner Production*, 170, pp.1536-1543.
- Vidhu, V. and Philip, D. (2015). Biogenic synthesis of SnO_2 nanoparticles: Evaluation of antibacterial and antioxidant activities. *Spectrochimica Acta Part A: Molecular and Biomolecular Spectroscopy*, 134, pp.372-379.
- Viswanathan, B. (2009). Nano materials. *Oxford: Alpha Science*, pp.2.1-2.11.
- Wu ZC, Zhang Y, Tao TX, Zhang L, Fong H (2010) Silver nanoparticles on amidoxime fibers for photo-catalytic degradation of organic dyes in waste water. *Applied Surface Science*257: pp. 1092-1097.
- Yagub, M., Sen, T. and Ang, H. (2012). Equilibrium, kinetics, and thermodynamics of methylene blue adsorption by Pine tree leaves. *Water, Air, & Soil Pollution*, 223(8), pp.5267-5282.
- Yu, L., Xi, J., Li, M., Chan, H., Su, T., Phillips, D. and Chan, W. (2012). The degradation mechanism of methyl orange under photo-catalysis of TiO_2. *Physical Chemistry Chemical Physics*, 14(10), pp.3589.
- Zollinger, H. (1989). Color chemistry: synthesis, properties and applications of organic dyes and pigments. *Leonardo*, 22(3/4), pp.456.

List of Websites Accessed

- Nano.gov. (2018). What is Nanotechnology? https://www.nano.gov/nanotech-101/what/definition [Date of Access 10.05.2018].

- trynano.org. (2018). The Future of Nanotechnology. http://www.trynano.org/about/future-nanotechnology [Date of Access30.04.2018].